

GPO PRICE \$ _____

CFSTI PRICE(S) \$ _____

Hamilton
Standard

U
DIVISION OF UNITED AIRCRAFT CORPORATION
A

Hard copy (HC) 3.00

Microfilm (MF) .75

ff 653 July 65

**DEVELOPMENT
OF
ALKALI METAL PEROXIDE
AND
SUPEROXIDE
BLOWN CERAMIC FOAMS**

**FINAL REPORT FOR THE PERIOD
JUNE 22, 1965 TO MARCH 15, 1966**

**E.W. BLOCKER AND R.D. PAUL
APRIL 5, 1966**

PREPARED FOR
NATIONAL AERONAUTICS AND SPACE ADMINISTRATION
GEORGE C. MARSHALL SPACE FLIGHT CENTER
HUNTSVILLE, ALABAMA 35812

(THRU)
(CODE)
15
(CATEGORY)

N66 31363
(ACCESSION NUMBER)

71
(PAGES)
CR-76406
(NASA CR OR TMX OR AD NUMBER)

FACILITY FORM 602

CONTROL NO. DCN 1-5-54-01186 (IF) & SI (IF)
CONTRACT NO. NAS 8-20089

PREFACE

This report was prepared by Hamilton Standard, Division of United Aircraft Corporation, under Contract NAS8-20089 (Development of Alkali Metal Peroxide and Superoxide Blown Ceramic Foams) for the George C. Marshall Space Flight Center of the National Aeronautics and Space Administration. The work was administrated under the technical direction of the Propulsion and Vehicle Engineering Laboratory, Materials Division of the George C. Marshall Space Flight Center with Mr. Vaughn F. Seitzinger (R-P&VE-MNC) acting as project manager.

ABSTRACT

A program has been conducted to develop a foam ceramic body for use as a thermal insulation. Specific areas investigated included the formulation of foam ceramic bodies, utilizing Li_2O_2 as the blowing agent, that achieve useful strength by a chemical bonding mechanism. The foam body was evaluated for physical/mechanical, thermal and optical properties.

A foam-in-place ceramic composed of zirconium phosphate bonded zirconia has been prepared and evaluated. The foam bodies exhibited good thermal and mechanical properties when tested in accord with accepted testing procedures.

TABLE OF CONTENTS

I INTRODUCTION

II FOAM CERAMIC DEVELOPMENT

A Materials Selection

B Coating Study

C Formulation and Development

D Optimization of Foam Ceramic

E Density Study

III EVALUATION

A Physical and Mechanical Properties

B Thermal Properties

C Optical Properties

IV SUMMARY

A Conclusions

B Recommendations

APPENDIX A

APPENDIX B

APPENDIX C

APPENDIX D

LIST OF TABLES

TABLE

I	Formulae of $ZrO_2 - H_2PO_3F$ Bodies
II	Formulae of $ZrO_2 - P_2O_5$ Bodies
III	Formulae of Modified $ZrO_2 - H_2PO_3F$ Bodies
IV	Observed Weight Change of Z59 Foam
V	Formulae of Bodies with Unclassified Additives
VI	Calculation of Closed Pore Volume - Z76 Foam
VII	Experimental Density Values of Z76 Foam
VIII	Modules of Rupture (Z76 Foam)
IX	Modules of Rupture (Z76 Foam)
X	Compressive Strength (Z76 Foam)
XI	Apparent Thermal Conductivity (Z76 Foam)
XII	Property Data for Z76 Foam Ceramic

LIST OF ILLUSTRATIONS

FIGURE

- 1 Comparison of Z76 Foam Bodies
- 2 Z76 Foam Ceramic Body
- 3 Photomicrograph of Z76
- 4 Photomicrograph of Z76
- 5 Foam Ceramic Shapes
- 6 Modules of Rupture Fixture
- 7 Thermal Stability of Z76
- 8 Z76 After Melting Point Determination
- 9 Thermal Conductivity Details

DEVELOPMENT OF ALKALI METAL
PEROXIDE AND SUPEROXIDE BLOWN
CERAMIC FOAMS

I. INTRODUCTION

This is the final report under NASA contract NAS8-20089, for the development of alkali metal peroxide and superoxide blown ceramic foams.

The tremendous advances made in the entire area of aerospace propulsion systems have created urgent requirements for inorganic insulation materials with the inherent capability of insulating at temperatures of plus 3000°F. The present generation of high specific impulse engines generates severe radiative and convective heating envelopes as well as high vibratory stresses. These conditions dictate the use of inorganic insulators that must fulfill specific requirements such as, high melting temperatures, insulating efficiency, oxidation resistance, and high mechanical strength. These general requirements may be used to define the properties of an ideal insulating material for aerospace vehicles. The insulating media must display low density and thermal conductivity, good thermal shock resistance, high melting point and mechanical strength.

A specific objective of this program was the development of improved insulating, i.e., lowered thermal conductivity, materials. It was proposed that a foam ceramic body, blown by oxygen gas, could be formulated to produce oxygen filled, closed pores within the ceramic matrix. The resultant foam body is expected to provide lowered thermal conductivity as compared to current gaseous blowing agents (hydrogen). The values below confirm this assumption.

oxygen @ (100°C)	7.6×10^{-5} cal/cm ² -sec/°C-cm
hydrogen @ (100°C)	54.7×10^{-5} cal/cm ² -sec/°C-cm

Cast ceramic bodies, composed of chemically-blown and chemically-bonded zirconia foams, were formulated and evaluated for their physical and mechanical, thermal, and optical properties.

II. FOAM CERAMIC DEVELOPMENT

A. Materials Selection

The concept of a chemically-foamed and bonded ceramic body was not unique with this facility. However, preliminary efforts were conducted prior to the contract award and certain conclusions were apparent. This background information was utilized in the selection of materials for investigation and enables the investigator to categorize the materials as:

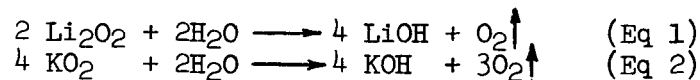
- foaming agents
- refractory media
- binders
- modifiers

These four material categories are essential to the development of a foam ceramic body and must be capable of forming a homogeneous mixture.

1. Foaming Agent

The use of alkali metal peroxides or superoxides as foaming agents was specified in the contract.

The primary use of these materials has been for air revitalization and self contained breathing equipment (References 1 and 2). The usefulness of peroxides and superoxides in the above applications is dependent upon the release of O₂. The reaction of two materials is shown below.



Lithium peroxide and potassium superoxide both readily liberate oxygen, are compatible with ceramic materials, and may readily be reduced to the stable oxide.

2. Refractory Media

The useful temperature capability specified for the foam ceramic is 3000 + °F. Accordingly it is very desirable to utilize inorganic materials with inherently high melting points (≈ 4000°F) to minimize any eutectic or degrading effect produced in the composite body.

Ceramic materials are often classified in the following groupings.

- | | |
|----------|----------|
| Carbides | Borides |
| Graphite | Oxides |
| Nitrides | Sulfides |

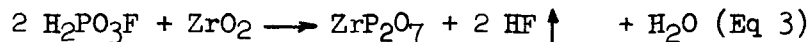
Carbides, graphite, and nitrides all share a common limitation; poor oxidation resistance. Borides are currently being investigated for various usages but comparatively little experience is available. Sulfides are seriously limited by chemical instability. This leaves the various oxide or mixed oxide materials for consideration. The following series of oxides all melt above 4500°F, are oxidation resistant, and chemically stable.

Beryllia (BeO)	Hafnia (HfO ₂)
Calcium (CaO)	Magnesia (MgO)
Zirconia (ZrO ₂)	Thoria (ThO ₂)

Zirconia has been utilized in the preparation of refractory ceramic coatings in which the useful strength and temperature resistance were achieved by chemical bonding (Reference 3, 4, & 5). The primary refractory media was zirconia.

3. Binder

Normal techniques of fabricating ceramic bodies utilize a vitreous or sintered bond. High temperature chemical bonds are in limited use. This program is dependent upon the use of low temperature chemical bonds. A listing of the chemical bonding systems used in conjunction with zirconia is given in Reference 6. The most promising material was a modified phosphoric acid (monofluophosphoric, H₂PO₃F). Edlin, in his work on the bonding reaction mechanism of ZrO₂/H₂PO₃F, has developed reaction equations (Ref. 5). The final equation is shown below.



Zirconium phosphate, ZrP₂O₇, dissociates to the zirconyl compound, (ZrO)₂ P₂O₇, at 2822°F with loss of P₂O₅ as a vapor (Reference 7). The dissociation reaction does not cause degradation of the bonded materials, as shown by the use of bonded zirconia coatings that exhibit capabilities in excess of 4000°F (Reference 8).

4. Modifiers

The production of chemically-bonded ceramics requires additives to assist in the reaction process. Likewise, foam bodies of all categories utilize foam stabilizers. Therefore, modification agents will undoubtedly be required but the selection was dependent upon laboratory work.

B. Coating Study

The foaming agents must be dispersed uniformly in the ceramic slurry to achieve maximum blowing effect and uniform pore structure. The achievement of a uniform dispersion is contingent upon the use of

finely divided powders (-35 mesh size). The reaction rate of powdered alkali metal peroxides and superoxides is reported to be rapid, and initial experiments during this program confirms this. A rapid reaction rate will result in poor blowing efficiency and non uniform pore structure.

Attempts were made to apply a degradable coating to the powdered foaming agent. This consisted initially of spraying a thin aqueous slurry of ZrO_2 upon the blowing agent. A charge of KO_2 was placed in a rotating cylinder. The rotational speed was adjusted to provide a tumbling action for the KO_2 . The spray was directed to impinge a semi-dry spray pattern of the slurry, upon the KO_2 grains.

In all instances reaction and liberation of O_2 was noted when the slurry impinged on the KO_2 . A heat lamp was positioned to warm slightly the surfaces of the KO_2 ($\approx 100-110^\circ F$) and thereby promote a slight interaction or adhesion of the coating. This did not eliminate the reaction.

Composite powders have been produced by intimate mixing of two materials. KO_2 and dry ZrO_2 powders were ball milled together. The resultant mixture was very viscous and appeared to have liberated the available oxygen.

Communication with the supplier of KO_2 (Reference 9) indicated that coating of peroxides or superoxides, while feasible, was a difficult problem. During this coating study, the development effort was conducted concurrently. Results of the development and formulation of foam ceramic bodies show that a coating was not essential, therefore, this effort was aborted.

C. Formulation and Development

1. General

The objective of this program was the development of chemically-foamed and chemically-bonded foam ceramic bodies. A supplemental requirement was the development of optimum properties and low temperature ($\approx 500^\circ F$) curing characteristics. The scope of this program was restricted to material development and there was no effort directed toward the establishment of an application system, i.e., foaming material upon substrates, adhesion, etc.

The materials selected for investigation will result in a foam ceramic body that may be described as a zirconium phosphate bonded zirconium oxide porous body with trace quantities of modifiers. The mechanics of producing this body are summarized, in a general fashion, below.

The dry ingredients are blended intimately and subsequently mixed

thoroughly with the liquid materials. The resulting slurry is agitated for a sufficient time to allow the evolution of the HF reaction product shown in Equation 3. The foaming agent and modifiers are added and thoroughly mixed. The slurry is cast immediately into molds and cured.

The molds are rigid enclosures with a tightly fitting cover. The use of a fully restrained blowing techniques enhances the uniformity of the foam structure. Mold materials used include aluminum, stainless steel, wood and plastic. A fluorocarbon, resin based mold release agent permits easy release of the cast body and inhibits attack upon the mold case.

Drying and curing the foam is related closely to the foam properties. The cast slurry was maintained at room temperature for sufficient time to complete the foaming action. Curing was accomplished using a conventional laboratory oven. The cure cycle could also be done by infra red lamps or other heat sources. Curing at 250-300°F produced a strong rigid body. However, it was necessary to post cure the body at 500°F to produce the final conversion to ZrP_2O_7 . The post cured body was insoluble in water.

2. Zirconia - H_2PO_3F System

The zirconia powder utilized in this series was calcium oxide stabilized and procured in -325 mesh fractions. Prior experience has shown that a blending of mesh sizes is beneficial to property values. For the purpose of this study it was decided to use one mesh fraction to minimize the quantity of formulations required to develop a uniform foam ceramic body. Original plans called for subsequent development effort utilizing various mesh size blends but lack of time prohibited this work.

The formulation of zirconia - H_2PO_3F foam ceramic bodies is shown in Table I. The basic reaction, shown in Equation 3, does not indicate the action of the $NH_4H_2PO_4$ additive. While the chemistry is not understood fully, it has been shown that ammonium dihydrogen phosphate serves as a retardant to prevent early setup of the slurry. Stoichiometric ratio is achieved with 2 mols of H_2PO_3F for each mol of ZrO_2 . An excess of ZrO_2 was utilized in formulations Z1 through Z18, to develop the ZrP_2O_7 bonded ZrO_2 matrix. This series of formulations was used to evaluate the effect of type and quantity of foaming agent, the ratio of acid to water, and the ratio of liquid to dry phases.

The majority of this series exhibited foaming of some degree. Z13 setup and hardened during mixing; Z18 did not setup after curing and Z16 released large quantities of steam during the cure cycle. The steam forced uncured material from the mold. Z16 was formulated with an excess of water that accounts for steam

TABLE I
FORMULAE OF $ZrO_2 - H_2PO_3F$ BODIES

Foam No.	ZrO ₂	NH ₄ H ₂ PO ₄	Al	K ₂ O	Li ₂ O	Composition			Starch	H ₂ PO ₃ F	H ₂ O	Kasil #1	Density g/cc	Remarks
						CaO	SiO ₂	CaO ₃						
Z1	200	18	0.8	—	—	—	—	—	—	36	26	—	—	fair poor structure
Z2	200	18	0.8	—	—	—	—	—	—	46.5	18.5	—	—	slow foam action, fair structure
Z3	300	27	—	1.5	—	—	—	—	—	54	39	—	—	premature foaming, no evidence of foam in body
Z4	50	4.5	0.3	—	—	—	—	—	—	15	5	—	—	body cracked during heat treatment
Z5	300	27	—	3	—	—	—	—	—	54	39	—	—	immediate set up, poor body
Z6	300	27	—	3	—	5	—	—	—	50	50	—	1.42	fair body structure
Z7	400	36	—	4	—	6.5	—	—	—	66.5	66.5	—	1.67	fair body structure
Z8	300	27	—	5	—	7.5	—	—	—	60	40	—	—	slight foam action
Z9	200	18	—	—	3.5	2.5	—	—	—	45	30	—	0.9	violent foaming, very porous body
Z10	200	18	—	—	3	2.5	—	—	—	45	30	—	0.93	fair pore volume, no cracks
Z11	200	18	—	—	2.5	2.5	—	—	—	45	30	—	1.0	poor foam rise
Z12	225	20	—	—	3.4	2.8	—	—	—	51	34	—	—	poor foam uniformity
Z13	225	20	—	—	4	2.8	—	—	—	51	34	—	—	set up in mixing vessel
Z14	225	20	—	—	3.4	2.8	—	—	—	51	45	—	1.01	exterior surface good, blow holes on interior
Z15	225	20	—	—	4	2.8	—	—	—	51	45	—	1.14	poor uniformity
Z16	225	20	—	—	4	2.5	—	—	—	15	80	—	—	blew out of mold, no set up
Z17	225	20	—	—	4	2.5	—	—	—	25	70	—	—	set up hard, poor rise
Z18	300	26	—	—	5.5	2.5	—	—	—	45	70	—	—	friable body, fair structure
Z19	250	30	—	—	4.5	3	—	—	—	158.5	10	—	—	violent foam rise, exotherm caused immediate setup
Z20	150	18	—	—	2.7	1.8	—	—	—	95.6	6	—	—	violent foam rise, blow holes normal to direction of rise
Z21	75	9	—	—	0.8	0.9	—	—	—	47.5	3	—	—	similar to Z20 with smaller pores
Z22	75	9	—	—	0.5	0.9	—	—	—	47.5	3	—	—	fairly uniform structure
Z23	75	9	—	0.5	—	0.9	—	—	—	47.5	3	—	—	fair structure
Z21a	100	12	—	—	1	1.2	—	—	—	63.2	4	—	—	poor foam rise
Z21b	150	18	—	—	1.6	1.8	—	—	—	95	6	—	—	foam rise doubled slurry volume, fair structure

TABLE I (CONT.)
FORMULAE OF ZrO₂ - H₂PO₃F BODIES

Foam No.	ZrO ₂	NH ₄ H ₂ PO ₄	Al	K ₂ O	Li ₂ O	Composition			Starch	H ₂ PO ₃ F	H ₂ O	Kasil #1	Density g/cc	Remarks
						CaCO ₃	SiO ₂							
Z21c	200	24	—	—	2	—	2.4	—	—	126.4	34	—	—	good foam rise - fair structure
Z9a	300	27	—	—	5.25	—	3.75	—	—	67.5	45	—	—	discarded
Z9b	150	13.5	—	—	3.5	—	2.5	—	—	45	30	—	—	good structure, cycled to 1500°F with slight cracking
Z9c	150	13.5	—	—	2.6	—	1.9	—	—	33.7	22.5	—	—	good structure
Z9d	150	13.5	—	—	2	—	1.9	—	—	33.7	22.5	—	—	good structure
Z9e	150	13.5	—	—	2	—	1.9	—	—	55	—	—	—	blow holes
Z25	175	16	—	—	3.5	—	—	—	—	24.5	35	—	1.32	uniform structure, some closed cells
Z26	175	16	—	—	4	—	—	—	—	24.5	35	—	1.4	uniform structure
Z27	22	2	—	—	0.45	—	—	—	—	3.5	6	—	—	used for annular casting - poor foam
Z28	22	2	—	—	0.3	—	0.3	—	—	3.5	6	—	—	same as Z27
Z29	150	13.5	—	1	—	—	—	2	—	30	22	—	—	poor definition of pores
Z30	150	13.5	—	7	—	—	—	2	—	30	20	—	—	microscopic pores plus pores 1/16 diameter
Z31	150	13.5	—	—	—	8	—	—	—	30	20	—	—	discarded
Z32	150	11	—	—	—	3	—	—	—	30	20	—	—	porous body - non uniform
Z33	150	—	—	—	—	3	—	—	—	10.5	30	—	—	porous body - non uniform
Z34	128.5	—	—	—	2	—	—	—	—	—	—	67.5	—	slight foaming - friable
Z35	53	—	—	1	—	—	—	—	—	—	—	23	—	large pores
Z36	53	—	—	1	—	—	—	—	—	—	—	12.8	—	no foam body
Z37	53	—	—	1	—	—	—	—	—	—	—	18	—	very slight porosity
Z38	53	—	—	—	—	1	—	—	—	—	—	16.6	—	no evidence of foam
Z39	159	—	—	3	—	—	—	—	—	—	—	69	—	slight porosity
Z39-1	260	—	—	5	—	—	—	—	—	—	—	113	—	no foam action

generation. The compositional variations in Z13 and Z18 do not explain their failure, this is attributed to variation in mixing. The remainder of the series exhibited non uniform pore sizes and contained large voids. The foam structure indicated that the foam agent was not dispersed thoroughly and the reaction was too rapid.

Stoichiometric ratios of H_2PO_3F and ZrO_2 were used in Z19 through Z23 to develop a ZrP_2O_7 body. The variables were those noted for the previous series. The cured bodies exhibited some degree of foaming, although the pore uniformity was poor.

The series Z21a, Z21b and Z21c were formulated in the same ratio of Z21. Z21a as a control, Z21b and Z21c were used to evaluate mixing modifications. The mixing sequence was altered for Z21b, and Z21c was mixed in a Waring blender. No significant advantage was realized.

During the previous mixing operations an exothermic reaction was observed. This was considered as a factor in the poor foaming characteristics. A cooling water bath was used to either inhibit the exotherm or minimize the heat retention in the slurry. Series Z9a through Z9e (ZrP_2O_7) were prepared to investigate this theory. The resultant slurries were more stable and had longer pot life. The cured foam structure appeared somewhat better.

Micron sized SiO_2 was used in Formulations Z6 through Z23 as a foam stabilizer. The results did not appear promising and the next series eliminated SiO_2 . Z25 through Z33 were ZrP_2O_7 bonded ZrO_2 . Foam stabilizer was not included in Z25 through Z27 and Z31 through Z33, corn starch was added to Z29 and Z30, while Z28 had SiO_2 as a control. The series was mixed in a cooling bath and the mixing sequence was modified. A slurry consisting of all materials except the foam agent and stabilizer was prepared and aged for time periods of 15 to 30 minutes. The remainder of materials were added mixed and the slurry cast. The pore structure of the cured bodies was greatly improved although the pores were interconnected. The open pores in Z25 was approximately 65% of the body volume. Microscopic examination revealed hemispherical depressions that appeared to be isolated pore sites. A slurry with low viscosity could develop closed pores and the oxygen pressure inside the pore may rupture the pore wall, thus creating interconnected pores.

A series was formulated with a higher viscosity to evaluate this theory. Z34 through Z39 can be described as a silicate bonded zirconia. The cured bodies appeared to possess closed pore structure although it was non-uniform. The apparent strength of the silicate bond did not compare with that obtained from the H_2PO_3F developed phosphate bond.

The results of this series of evaluations indicate that viscosity of the slurry is a major criteria for optimum foam ceramic formulations. It was assumed that thixotropic materials would possibly be of benefit.

3. Phosphate Bonded Bodies

The series P1 through P6 consisted of a cursory evaluation of phosphate binders based upon a patent granted to Vukasovich, Wickliffe and Johns (Reference 10). The formulations are shown in Table II. Z42 and Z43 are included in this series as they are modifications of the phosphate bond system. The results of this series were disappointing in that the pore structure and strength characteristics were poor.

TABLE II

FORMULAE OF $ZrO_2 - P_2O_5$ BODIES

Materials	Formulation (parts by weight)					
	P1	P2	P3	P4	P5	P6
Alkaphos CE	25	60	—	—	—	—
$ZrO_2 \cdot 2P_2O_5 \cdot X H_2O$ *	—	—	18.2	125	—	—
Al_2O_3 T61	—	—	—	—	248	—
ZrO_2 Zircoa B	—	—	—	—	—	45
$CaO \cdot SiO_2$	25	25	3.7	—	—	—
Wollastanite	—	—	—	25.4	—	—
$CaCO_3$	2.5	2.5	—	—	—	—
Al	—	—	—	—	0.2	0.1
Li_2O_2	—	—	0.5	3.5	—	—
Starch	—	—	—	—	4.8	2.4
H_3PO_4	—	—	—	—	92	46
H_2O	65	46	—	—	54.8	27.4

*Prepared in laboratory

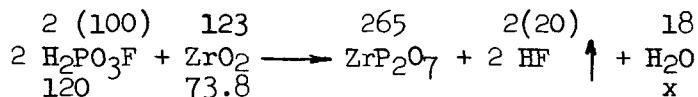
ZrO_2	40 g
P_2O_5	92 g
H_2O	60 g

4. Modified Zirconia - H₂PO₃F System

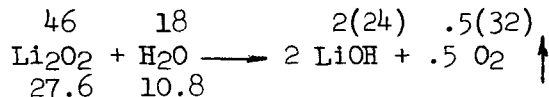
The previous work with the ZrP₂O₇ bonded matrix material has shown erratic results for pre size, uniformity, and foam reaction rates. However, this bonding technique produces hard, strong bodies when cured at low temperatures. This system has been designed to use the H₂PO₃F - ZrO₂ reaction, with an excess of ZrO₂, to evaluate the foam reaction. Specific areas to be investigated involve a more viscous slurry and/or thixotropic phenomena. The formulation of this foam ceramic system is shown in Table III.

Z44 through Z47 were used to evaluate bentonite and Baymal as a means of achieving viscosity. A wetting agent was incorporated in Z44 and Z45. Z46 and Z47 did not contain the acid binder, this allowed evaluation of the Baymal - ZrO₂ interaction. These four slurries were prepared primarily to enable observation of the slurry characteristics and valuable information was obtained. The use of both bentonite and Baymal produced a thicker slurry that appeared to provide efficient entrainment of the O₂ blowing media. Baymal is a colloidal aluminum oxide material with the nominal composition AlOOH.

The Li₂O₂ reaction rates produce the best results with respect to controlled foaming action. The majority of succeeding formulations contain Li₂O₂ as the foam agent. It is desirable to work with controllable foam reactions, however, it is also desirable to maintain high foaming efficiency. Equations 1 and 2 readily show KO₂ as the more efficient blowing agent (2 mols Li₂O₂ → 1 mol O₂; 2 mols KO₂ → 1.5 mol O₂). Therefore, KO₂ has been included in the present series formulation. Z48 through Z62 used Baymal (AlOOH) as a thickening agent in the ZrP₂O₇/ZrO₂ slurry. Water additions were eliminated to reduce the rapidity of the Li₂O₂ reaction. This decision was based upon the availability of sufficient water from the acid-zirconia reaction, as indicated below.



120 grams of H₂PO₃F reacted stoichiometrically with 73.8 grams of ZrO₂ yields 10.8 grams of water.



The available H₂O (10.8 g) would theoretically react with 27.6 grams of Li₂O₂; considerably more Li₂O₂ than required. One gram of Li₂O₂ releases 0.35 gram of O₂, or 240 cubic centimeters of

TABLE III
FORMULAE OF MODIFIED $ZrO_2 - H_2PO_3F$ BODIES

Foam No.	Composition										Density g/cc	Remarks
	ZrO ₂	NH ₄ H ₂ PO ₄	K ₂ O	Li ₂ O ₂	Baymail	Bentonite	Wetting Agent	H ₂ PO ₃ F	H ₂ O			
Z44	31	—	—	2	—	10	0.5	50	20	no setup		
Z45	31	—	—	2	—	10	0.5	50	—	poor setup		
Z46	150	—	—	0.5	5	—	—	—	47	no setup		
Z47	40	—	—	1	2.4	—	—	50	—	immediate setup - very porous		
Z48	123	—	—	0.8	4	—	—	100	—	incomplete rise, setup hard, some closed cells		
Z49	147.6	—	—	1	4.8	—	—	120	—	similar to Z48		
Z50	147.6	—	—	1	4.8	—	—	120	—	≈ 35% rise in 45 minutes, foam structure variable		
Z51	147.6	—	—	2	—	—	—	120	—	setup hard, foam gradient top to bottom		
Z52	147.6	—	—	1.5	4.8	—	—	120	—	cast into plaster mold, no setup		
Z53	147.6	—	—	2	4.8	—	—	120	—	set up hard, gradient top to bottom, density at bottom 1.3 g/cc		
Z54	147.6	—	—	2.5	4.8	—	—	120	—	similar to Z53, more uniform gradient		
Z55	147.6	—	1.5	—	4.8	—	—	120	—	very high exotherm, hard body		
Z56	147.6	—	—	2	4.8	—	—	120	—	slow setup, fair body		
Z57	147.6	—	—	—	4.8	—	—	120	—	slow setup, fair body		
Z58	73.8	—	—	0.25	2.4	—	—	60	—	slight rise		
Z59	73.8	—	—	0.5	2.4	—	—	60	—	slight rise, some foam structures		
Z60	73.8	—	—	0.75	2.4	—	—	60	—	viscous mix, poor body		
Z62	73.8	—	—	1	2.4	—	—	60	—	fair body		
Z63	110.7	—	—	—	8	—	—	180	—	setup in mixer		
Z64	73.8	—	—	1	2.4	—	—	60	—	fair body, some closed cells		
Z65	73.8	—	—	—	4.8	—	—	120	—	good structure, foam bodies from Z65 to Z76 are all very similar		
Z66	147.6	—	—	1	4.8	—	—	120	—			
Z67	138.8	—	—	1	3.5	1	—	120	—			
Z68	138.8	11.5	—	2	3.5	1	—	120	—			
Z69	138.8	11.5	—	1.5	3.5	1	—	120	—	foam bodies all good, uniform structure, closed cells		

TABLE III (CONT.)
 FORMULAE OF MODIFIED $ZrO_2 - H_2PO_3F$ BODIES

Foam No.	Composition										Density g/cc	Remarks
	ZrO_2	$NH_4H_2PO_4$	KO ₂	Li_2O_2	Baymail	Bentonite	Wetting Agent	H_2PO_3F	H_2O			
Z70	147.6	13	—	1.5	3.5	1	—	120	—	—	foam bodies all good, uniform structure, closed cells	
Z71	147.6	13	—	1.5	4	1.5	—	120	—	—	foam bodies all good, uniform structure, closed cells	
Z72	147.6	7.4	—	1	4	1.5	—	120	—	1.3	foam bodies all good, uniform structure, closed cells	
Z73	147.6	10.2	—	1	4	1.5	—	120	—	—	foam bodies all good, uniform structure, closed cells	
Z74	147.6	10.2	—	1	4	4.5	—	120	—	—	foam bodies all good, uniform structure, closed cells	
Z75	147.6	10.2	—	3	4	4	—	120	—	—	foam bodies all good, uniform structure, closed cells	
Z76	147.6	10.2	—	2	4	2	—	120	—	—	foam bodies all good, uniform structure, closed cells	

O₂ at standard temperature and pressure.

The mixing technique was modified during this series to provide a more thorough release of HF gas from the slurry. Stoichiometric ratios of H₂PO₃F and zirconia were mixed for periods of time varying from 15-45 minutes. Gas evolution was observed and when the bubble formation ceased, an excess of ZrO₂ was added to the slurry. The thickening agent was added and blended thoroughly. Li₂O₂ added, dispersed and the slurry cast into molds for subsequent curing. Z53 deviated slightly from this sequence. The slurry was placed in a Waring blender and the Li₂O₂ dispersed at high speed mixing. The formulation was cured as before. The resultant foam ceramic bodies were very promising; the pore structure was somewhat uniform and evidence of closed cells was apparent. The apparent bulk density of Z53 and Z54 was 0.90 and 0.96 g/cc, respectively. Z59 was checked for density properties using the ASTM standard C20-46. The calculated density was 1.5 g/cc with 59.3% open pores. The boiling action specified in ASTM was believed to force water through microscopic openings into otherwise closed pores. To evaluate this theory, the Z59 block was dried and static soaked in water. Table IV shows the weight change observed.

TABLE IV
OBSERVED WEIGHT CHANGE OF Z59 FOAM
STATIC WATER SOAK

Time (hrs)	Cumulative Time (hrs)	ΔW (g)	Cumulative ΔW (g)
24	24	+ 1.58	1.58
24	48	+ 0.20	1.78
24	72	no change	1.78
24	96	no change	1.78
72	168	+ 0.42	2.20
168	336	+ 0.40	2.60
96	432	no change	2.60

The total weight change was 2.60 g compared to 3.5 g in boiling water. This shows an apparent increase in closed pores.

The series Z63 through Z76 were very similar to the preceding

series and was designed to provide additional information on mixing procedures, additives, and foam characteristics. This series represented an improvement in the foam ceramic body, with both Z72 and Z76 exhibiting very good pore structure. The bulk density of Z72 was 1.3 g/cc.

5. Investigation of Additional Modifiers

The ZrP_2O_7 bonded ZrO_2 foam ceramic, as characterized by Z72 and Z76, appeared to offer the best opportunity to fulfill the contractual objective. Various slight modifications were advanced and to evaluate these, series Z77 through Z84 was formulated. This series is shown in Table V. Bulk densities obtained range from 0.48 to 1.12 g/cc depending upon the formulation. The bodies were very weak and friable. This effort was discontinued.

TABLE V

FORMULAE OF BODIES WITH UNCLASSIFIED ADDITIVES

Material	Formulation (parts by weight)									
	Z77	Z78	Z79	Z80	Z81	Z82	Z82a	Z82b	Z83	Z84
ZrO ₂	65	147.6	147.6	147.6	147.6	147.6	147.6	147.6	147.6	147.6
NH ₄ H ₂ PO ₄	5	5	5	5	5	5	5	5	5	5
Li ₂ O ₂	1	2	2	1	2	2	2	2	2	2
KO ₂	---	1	---	---	---	---	---	---	---	---
CaCO ₃	---	---	---	---	---	---	---	5	---	---
Bentonite	1	1	1	1	1	1	1	1	1	1
AlOOH	---	4.8	5	5	5	5	5	5	5	5
CaO·SiO ₂	---	---	---	---	---	---	---	9.2	---	---
KMnO ₄	1	---	---	---	---	---	---	---	---	---
Alkaphos CE	---	---	---	---	---	---	31.8	31.8	---	---
H ₂ PO ₃ F	30	17.8	60	60	45	55	55	55	50	55
H ₃ PO ₄	---	---	---	---	---	---	---	---	---	30
H ₂ O ₂	---	---	---	---	---	---	---	---	10	---

TABLE V (CONT)

FORMULAE OF BODIES WITH UNCLASSIFIED ADDITIVES

Material	Formulation (parts by weight)									
	Z77	Z78	Z79	Z80	Z81	Z82	Z82a	Z82b	Z83	Z84
H ₂ O	12.5	70	80	50	70	100	100	130.8	70	70
Density (g/cc)	---	---	1.19	---	1.05	0.48	0.87	---	0.98	1.12

6. Discussion

The development effort described in the foregoing sections has shown the feasibility of utilizing a ZrP₂O₇ bonded ZrO₂ as the matrix material for a foam ceramic blown with Li₂O₂. The most promising formulations exhibit good strength properties, appear to possess comparatively uniform pore structure and a fair volume of closed pores. The reproducibility of the foam is poor and the desired properties are not fully developed. Z72 and Z76 were selected for optimization.

D. Optimization of Foam Ceramic

Foam ceramic formulations Z72 and Z76 have demonstrated significant value, although the properties are not consistently uniform. These two formulations were selected for an optimization study. Both formulations are defined as, "zirconium phosphate bonded zirconia bodies utilizing lithium peroxide as the source of gaseous oxygen for development of a foam structure".

The initiation of this study coincided with a series of foam body failures. The slurry did not react in the previously observed manner, a completely random pattern emerged. Slurries set up during initial mixing stages, slurries did not set up, and foam bodies exhibited large blow holes. After a reevaluation of the entire concept, it was theorized that the acid was at fault. The acid is anhydrous but not 100 per cent H₂PO₃F. An equilibrium exists between H₃PO₄ (or HPO₃), HPO₂F₂ and H₂PO₃F, where H₂PO₃F is present to the extent of approximately 80 weight per cent. It was established (Reference 11) that the present lot was low in fluoride concentration. The cumulative fluoride level is maintained in the 18.5-19 weight per cent range. The determination of fluoride content normally is accomplished by means of the Willard and Winter distillation technique and a control check method is not available. The manufacturer's information enabled correction of the fluoride deficiency by an addition of hydrofluoric acid. This action produced acceptable foam ceramic bodies. The difficulties

encountered confirm Edlins work (Ref. 5) in which he concluded that the presence of fluoride radicals was essential to the bonding mechanism. A program delay resulted from this difficulty and it was decided to limit future work to the Z76 formulation.

A review of the developmental and initial optimizing work indicated that the primary critical area of the process was the mixing of the slurry. This assumes that all reactants are within specification. A process chart was prepared that shows twenty-one plateaus, during mixing, that can affect the foam ceramic body.

Experimental work has shown that the initial mixing of acid and zirconia primarily controls the slurry preparation. Equation 3 shows that the formation of ZrP_2O_7 is accompanied by the release of HF. Exploratory work has demonstrated that incomplete evolution of the HF results in a secondary reaction (not defined) that is detrimental to the formulation. Periods of mixing were varied from five minutes to greater than one hour. Short mixing times resulted in uncontrolled foam reaction. Figure 1 shows a comparison of foam Z76 bodies formulated by various mixing times.

The formation of ZrP_2O_7 was accompanied by an exothermic heat of reaction. Small slurry volumes (≈ 150 cc) were relatively unaffected. Sufficient heat was developed in large slurry volumes to cause degradation of the slurry and premature setup of the slurry. The use of a cooling water jacket during mixing minimized the heat build up and resulted in lower viscosity and smoother slurries. The water jacket also appeared beneficial in producing slurries that temporarily inhibited the subsequent $Li_2O_2 - H_2O$ reaction.

The secondary, or excess, ZrO_2 addition was not a source of trouble. The final additives, Li_2O_2 and bentonite, were a critical factor. Intimate, yet rapid, dispersion of the peroxide was shown to be essential. A mixing period of 60 seconds in an intensive mixer (Waring blender) produced the optimum result.

Initial curing of the cast slurry was also a potential source of foam structure failure.

Dense blue-grey, pungent fumes were observed with the cast slurry when the initial curing was too soon or the rates were too rapid. The fumes persist for approximately three minutes and are accompanied by a high exotherm. After the fumes subside the foam ceramic is hard and appears cured. This action frequently ruptures or produces blow holes in the body and is undesirable. The following postulate is advanced for this behavior. The slurry is metastable at room temperature and the Li_2O_2 is known to react with heat. The curing cycle accelerates the Li_2O_2 -water reaction rate and the additional temperature or a pressure build up is sufficient to bring about an irreversible reaction, establishing a stable phase.

To evaluate the exothermic heat and the pressure buildup a simple experiment was devised. A mold was modified to provide temperature and pressure take offs. Temperature was measured by a thermocouple immersed in the slurry and the pressure was read from a U tube manometer. The cast slurry and mold were placed on a hot plate to provide the heat required to initiate the exothermic reaction.

A slurry volume of 75-80 cm³ generated an exothermic reaction temperature in the range of 365-385°F. The measured vapor pressure developed over this slurry volume was 380 g/cm². The heat developed during the exothermic reaction was sufficient to set up the slurry into a hard body that can be removed from the mold case and further cured to 500°F to render insolubility. This reaction mechanism is believed to have merit for certain applications in which an external heat source is required to initiate the reaction.

This study has been successful in producing foam ceramic bodies that possess uniform pore structure and good pore distribution in the direction of foam rise and in a plane normal to the foam rise. Figure 2 shows a Z76 foam ceramic cut to exhibit internal structure. Figure 3 and 4 are photomicrographs of Z76 foam. Several foam ceramic shapes are shown in Figure 5.

E. Density Study

An important facet of the concept of alkali metal peroxide ceramic foam was the inclusion of closed pores in the foam matrix. The ASTM standard C20-46 is useful in determining the volume of the open pores and the volume of the impervious portion. Additional techniques are also available for determination of these properties. However, there is no provision for the determination of the closed pore volume. A technique was developed that utilizes the standard density-porosity test and a pycnometer density test.

The volume and bulk density of the impervious portion is determined after a soak period in water. The body is then dried to constant weight, crushed and sized. The powder density is obtained through the pycnometer test method (ASTM C-128). Assuming there are no voids within the impervious portion of the foam body, the density of this phase should approximate that of the crushed powder. If the powder density is greater than that of the impervious material, it is reasonable to assume that voids are included in the impervious portion as closed pores. The void volume, or per cent closed cells, can be calculated for the foam ceramic body. Table VI shows a calculation for a Z76 foam body.

TABLE VI
 CALCULATION OF CLOSED PORE VOLUME
 TYPICAL Z76 FOAM

Property		Method	Value
Dry Weight	D	ASTM C20-46	9.0 g
Saturated Weight	W	ASTM C20-46	10.6 g
Suspended Weight	S	ASTM C20-46	4.5 g
Volume - Exterior	V	W-S	6.1 cc
Volume - Apparent Impervious	V1	D-S	4.5 cc
Volume - Open Pore	V2	W-D	1.6 cc
Bulk Density	B	D/V	1.47 g/cc
Density - Impervious	B1	D/V1	2.00 g/cc
Powder Density	B2	ASTM C-128	2.98 g/cc
Volume - True Impervious	V3	D/B2	3.02 cc
Volume - Closed Pores	V4	V1-V3	1.48 cc
Open Pore Percentage		$(V2/V) 100$	26.2%
Closed Pore Percentage		$(V4/V) 100$	24.3%
Matrix Percentage		$V - (V2 + V4)$	49.5%

III. EVALUATION

The objective of this program was the development of a foam ceramic body suitable for use as a thermal insulation material for radiative and convective temperature extremes. A foam ceramic body was developed and optimized for use in the stated objective. The body has been characterized as to materials, processing history, and chemical composition. The efficiency of the foam reaction was studied and a visual examination established the pore uniformity and distribution. The optimized material must be evaluated to allow determination of qualitative values for physical/mechanical, thermal, and optical properties. The optimized foam body is designated Z76.

A. Physical and Mechanical Properties

1. Density

The density of the foam body can be controlled by using predetermined amounts of the slurry in a specific volume mold. Experience has demonstrated this technique, however, there was not sufficient data developed to permit establishing a schedule of volume to density. Table VII provides observed density values correlated with open and closed pore volume for several bodies cast from the Z76 formulation.

TABLE VII
EXPERIMENTAL DENSITY VALUES FOR Z76 FOAM

Bulk Density g/cc	Powder Density g/cc	% Open Pores	% Closed Pores	% Matrix	Mold Fill Volume %	Application
1.82	3.42	33.3	14	52.7	60	Compressive Strength
1.80	3.30	34.6	10.9	54.5	70	Thermal Conductivity
1.48	3.23	33	21.4	45.6	70	Thermal Conductivity
1.48	3.43	27.5	30.3	42.2	70	Thermal Conductivity
1.06	3.10	37.8	28	34.2	70	Experimental
1.17	3.03	26.8	34.4	38.8	60	Experimental
1.16	3.02	26.5	35	38.5	60	Experimental

TABLE VII (CONT)

EXPERIMENTAL DENSITY VALUES FOR Z76 FOAM

Bulk Density g/cc	Powder Density g/cc	% Open Pores	% Closed Pores	% Matrix	Mold Fill Volume %	Application
1.25	3.05	15.5	43.4	41.1	50	Experimental
0.97	3.06	37.6	30.7	31.7	60	Flexural Strength
0.96	3.05	43	25.4	31.6	60	Flexural Strength

2. Flexural Strength

The flexural strength was evaluated at room temperature, using a four point loading modulus of rupture technique. The support pins were spaced 2.50 inches apart. The loading pins were spaced 1.25 inch apart. The loading rate was 0.05 inch per minute, applied through a cone-pointed disc. Figure 6 shows the fixture and the broken specimens.

The test specimens were cut from two separate castings into a nominal size of 0.5 X 0.5 X 3.0 inches. Modulus of Rupture was calculated using the equation.

$$S_R = \frac{3 W (L_1 - L_2)}{2 B D^2}, \text{ where} \quad \text{(Equation 4)}$$

- S_R = Modulus of Rupture in psi
- W = Load in pounds at failure
- L_1 = Length of lower span in inches
- L_2 = Length of upper span in inches
- B = Breadth of specimen in inches at fracture
- D = Depth of specimen in inches at fracture

The constant values of L_1 and L_2 (2.50 and 1.25 respectively) permit the reduction of Equation 4 to:

$$S_R = \frac{1.875 W}{B D^2} \quad \text{(Equation 5)}$$

Results of modulus of rupture tests are shown in Tables VIII and IX. Scatter can be expected in modulus of rupture data for brittle ceramic materials, and the range of values does not appear excessive for the high porosity material. The extent of scatter pro-

vides an indication of the general quality of the material, such as uniformity of pore size.

TABLE VIII

MODULUS OF RUPTURE (Z76 FOAM)
 APPARENT DENSITY 0.97 g/cm³ APPARENT POROSITY 37.6%

Specimen	Breadth (in.)	Depth (in.)	Load (lb)	Modulus of Rupture (psi)
1-1	.456	.505	12.85	207
1-2	.453	.501	14.25	235
1-3	.498	.510	13.50	195
1-4	.497	.522	20.00*	277
Average				228.5
* Load beyond scale		Maximum deviation from average		+ 21% - 15%

TABLE IX

MODULUS OF RUPTURE (Z76 FOAM)
 APPARENT DENSITY 0.96 g/cc APPARENT POROSITY 43%

Specimen	Breadth (in.)	Depth (in.)	Load (lb)	Modulus of Rupture (psi)
2-8	.494	.503	18.60	279
2-9	.483	.504	15.65	239
2-10	.495	.520	17.40	244
2-11	.459	.528	15.20	223
Average				246.3
		Maximum Deviation from Average		+ 13% - 9%

3. Compressive Strength

The compressive strength was evaluated at room temperature using a Tinius Olsen Universal Testing Machine. The load was applied through a cone pointed disc. The test specimens were cut from one Z76 casting into a nominal size of 1 X 1 X 2 inches. Particular care was taken to keep the 1 X 1 inch faces parallel. Compressive stress was calculated using the equation.

$$\sigma = \frac{P}{A}, \text{ where} \quad \text{(Equation 6)}$$

σ = Stress in psi
 P = Total load in lbs
 A = Cross sectional area in in².

TABLE X

COMPRESSIVE STRENGTH (Z76 FOAM)
 APPARENT DENSITY 1.82 g/cc APPARENT POROSITY 33.3%

Specimen	Width (in)	Depth (in)	Area (in ²)	Total Load (lb)	Compressive Stress (psi)
1	.998	.972	.970	732	755
2	.999	.972	.971	750	772
3	.999	.944	.943	790	838
4	.999	1.018	1.017	572	562
Average					731.75
Maximum Deviation from Average					+ 15% - 23%

4. Thermal Shock Resistance

Blocks of Z76 foam ceramic, one inch thick, were used to evaluate the thermal shock resistance. The nominal block size was 2 X 4 inches. The evaluation procedure consisted of heating the block to a specific temperature in an electric resistance furnace operated in air; soaking at temperature for 20 minutes, removal from furnace and immediate shocking with a cold air blast. The test is considered severe; the cold air blast impinged upon one surface is effectively limited to a very small penetration into the body by low thermal conductivity. The back surface can only

be cooled by radiation and convection, thereby remaining very near the furnace temperature. The disparity in surface temperatures induces severe cooling stresses that were evidenced by bowing of the foam body. The bowing was accompanied by cracking and, in some instances, splitting of the body. Thermal shock tests were run at 1000, 1200, 1500, 2000 and 2500°F with similar results. Cracking was somewhat more severe with increasing temperature but even at 2500°F catastrophic failure did not occur. The thermal shock resistance of Z76, based upon this method of testing, must be evaluated as fair to poor.

It is believed that the thermal shock resistance can be improved by modification of the zirconia refractory grain. The zirconia phase consisted entirely of -325 mesh stabilized ZrO_2 , partially fused. The use of fully fused grain in a suitable blend of mesh sizes is expected to yield better thermal shock resistance.

During the thermal shock evaluation light grey fumes were observed at temperatures up to 1500°F. This concurred with observations made during the thermal conductivity and melting point tests. Specimens of Z76 foam, previously cured at 500°F for one hour, were subjected to annealing cycles to determine an optimum cure. An additional cure period of 5 hours at 500°F practically eliminated the fumes.

B. Thermal Properties

The thermal property evaluation was conducted by the United Aircraft Research Laboratories, a division of the United Aircraft Corporation. The results of the evaluation are summarized in the following paragraphs and the complete report is included as Appendix C.

1. Thermal Stability

Weight loss as a function of temperature was determined by heating a finely ground portion of Z76 in an electric resistance furnace with an air atmosphere. The cumulative weight loss, to approximately 2900°F, was 5.55%. The weight loss curve is shown in Figure 7.

The work is not a complete thermogravimetric analysis since the weight change rate between 80°F and 2156°F was not determined. The observed weight loss in this range is attributed to complete drying of the powder and volatilization of the HF gas. The abrupt change of slope at 2550°F is analagous to the literature report (Ref. 7) of dissociation of ZrP_2O_7 to $(ZrO)_2P_2O_7$ with a release of P_2O_5 as a vapor. The reported dissociation temperature is 2822°F compared to the observed temperature of 2552°F. This apparent discrepancy is attributed to the composite nature of the material. While this 2552°F point is considered the thermal stability point, experimental evidence indicates the foam body

can be used up to the melting point without catastrophic degradation. If the evolution of P₂O₅ fumes is objectionable, the foam body can be fired above the dissociation temperature prior to use.

2. Melting Point

The determination of the melting point of Z76 was conducted in an argon atmosphere within a tungsten resistance furnace. The specimens were supplied in an as-cast condition and were 0.5 inches in diameter and approximately 1.5 inches long. The melting temperature was determined by the temperature observed at the first formation of liquid. The melting point of Z76 was determined as 1835°C + 10°C (3335°F) in an argon atmosphere 4.5 psi above atmospheric pressure. Z76 test specimens, after the melting point determination, are shown in Figure 8.

3. Thermal Conductivity

A radial heat flow stacked-disc technique was utilized in the thermal conductivity determination. The test specimens and guard specimens were Z76 foam ceramic foamed in place to the required dimensions. Figure 9 shows the mold details and a typical test specimen.

The measured values of thermal conductivity for Z76 foam ceramic are shown in Table XI.

TABLE XI

APPARENT THERMAL CONDUCTIVITY (Z76 FOAM)
AVE DENSITY 1.59 g/cc

Mean Temperature		Thermal Conductivity	
°F	°C	Btu/hr °F-in/ft ²	Cal/sec °C-cm/cm ²
578.7	303.7	3.25	0.00112
871.9	466.6	3.37	0.00116
1068.1	575.6	3.77	0.00130
1244.3	673.5	4.06	0.00140
1404.0	762.2	4.24	0.00146
1524.7	829.3	4.27	0.00147
1553.5	845.3	4.5	0.00155

The preparation of thermal conductivity specimens was conducted during the time that difficulty was encountered in producing acceptable foam bodies. The foam ceramic structure used in the above tests was not the optimum that was developed later. A comparison of bulk density and pore volume shows that the conductivity specimens were nearly double the density of flexural samples with a decrease in porosity. It is proposed that the conductivity values would be enhanced if the optimum foam body had been developed prior to this evaluation.

C. Optical Properties

The evaluation of optical properties that characterize Z76 foam ceramics, was conducted by Pratt and Whitney Aircraft, a division of the United Aircraft Corporation. The evaluation included total hemispherical emittance at elevated temperatures. The Pratt and Whitney Aircraft report is included as Appendix D.

It was unfortunate that the preparation of test items, for optical property evaluation, coincided with the period in which difficulty in preparing acceptable foam bodies was experienced. Test items could not be fabricated to the desired configurations and alternate configurations had to be substituted.

1. Emittance

The total hemispherical emittance was measured at temperatures of 151°F and 317°F. The alternate specimen configuration severely limited the measurement technique and lack of time precluded further work. The measured values are shown below.

<u>Emittance</u>	<u>Temperature</u>
0.75	151°F
0.78	317°F

2. Discussion

The test equipment restrictions dictated the use of thin panels (< 1/4 inch) of the foam ceramic body. To achieve thicknesses of this order, it was necessary to cut panels from foam ceramic blocks. The resulting surfaces exhibited roughness and a large proportion of void spaces. This surface condition is considered as optically poor. It is postulated that the optical properties would be enhanced using as-cast surfaces, or a coating of unfoamed ZrP₂O₇ bonded ZrO₂.

VI. SUMMARY

This program was directed toward the development of a chemically-foamed, chemically-bonded refractory body designed for use as a thermally insulative media in convective and radiative heat environments. Basically the work has been limited to ZrO_2 grain bonded with H_2PO_3F ; a minor effort utilized phosphates and silicates as a binder.

An optimized foam ceramic body, designated Z76, has been developed and evaluated. The body is described as a stoichiometric ratio of ZrO_2 and H_2PO_3F that produces ZrP_2O_7 ; the use of excess ZrO_2 provides a ZrP_2O_7 bonded ZrO_2 structure. Study of the gross properties show a uniform pore distribution and a narrow range of pore sizes. The as-cast surface of the body exhibited a smooth (matte) skin that was hard, and penetrated by small diameter holes connected to internal pores. Cut surfaces of the body show hemispherical depressions that appear as closed cells. An interesting phenomenon was the arrangement of internal pores into a repeating hexagonal pattern. This has not been explained. The foam ceramic body is white with a tendency toward the typical zirconia buff color when heated to high temperature in air. Heating in argon exerts a reducing influence as indicated by the grey color developed.

The Z76 properties that have been evaluated are tabulated in Table XII.

TABLE XII
PROPERTY DATA FOR Z76 FOAM CERAMIC

Property Category	Value
1) Density Range	0.96 - 1.80 g/cc
2) Flexural Strength (Modulus of Rupture)	237 psi
3) Compressive Strength	731 psi
4) Thermal Shock Resistance	fair to poor
5) Melting Point	3335°F
6) Thermal Conductivity	4.5 Btu/hr °F in/ft ² at 1550°F
7) Emittance (Hemispherical)	0.78 at 317°F

A. Conclusions

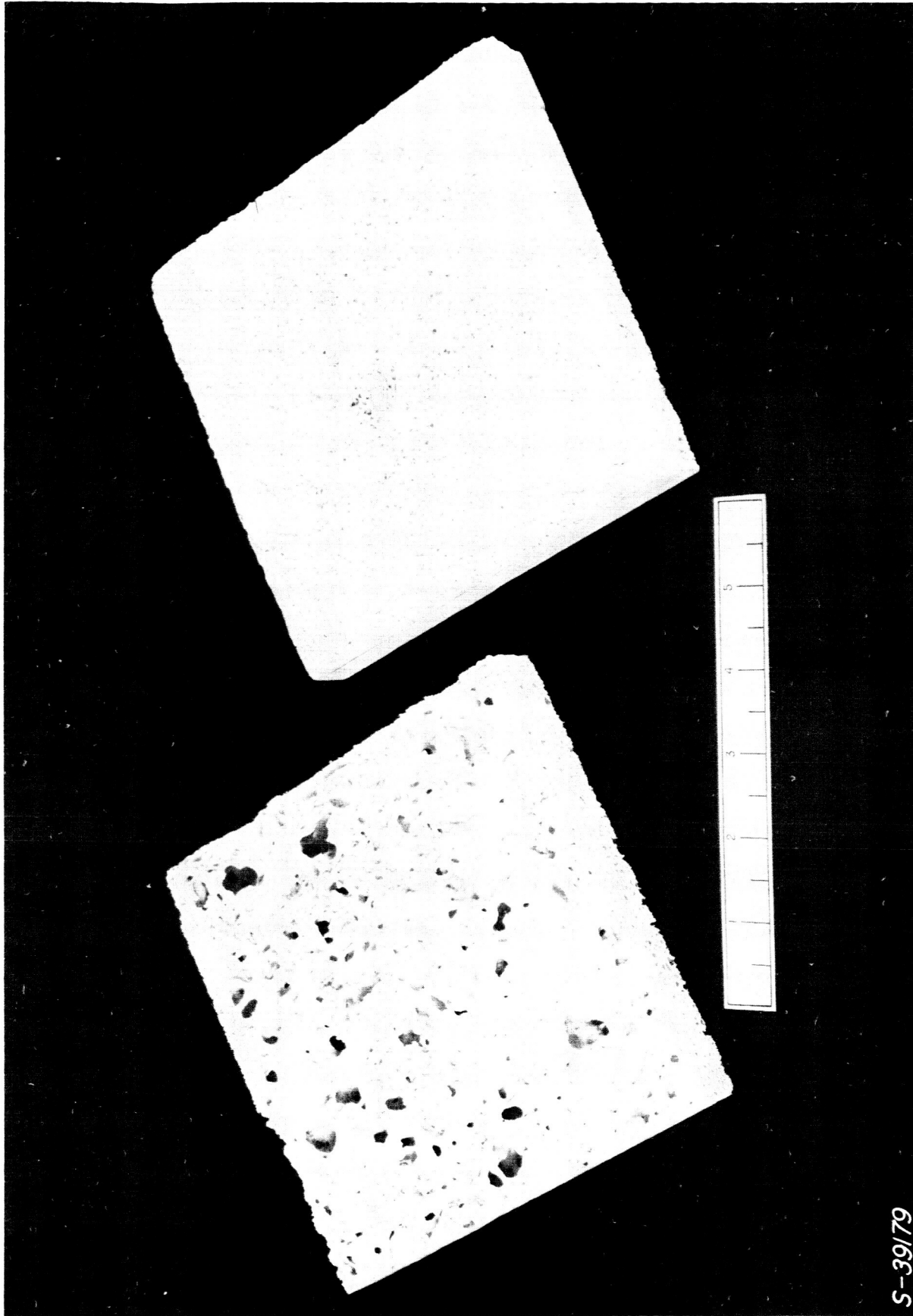
1. It is possible to utilize alkali metal peroxides and a chemical reaction bonding system to produce foam ceramic bodies for use as insulating media.
2. The foam agent (Li_2O_2) must possess a controllable reaction rate for maximum foaming efficiency.
3. The Z76 foam ceramic body developed under this program shows promise for use as a thermal insulation material.

B. Recommendations

1. The Z76 foam ceramic body should be further developed in the following areas:
 - a. establish a range of refractory grain mesh sizes to minimize shrinkage, thermal shock damage and provide better strength.
 - b. evaluate fully fused refractory grain to minimize shrinkage and thermal shock damage.
 - c. evaluate zirconia grain stabilized with other materials (Y_2O_3 , Ti, etc.).
2. Study additions of fiber or whisker materials to the basic slurry as a means of enhancing the mechanical properties of the foam ceramic.
3. Further evaluation of the optical properties is essential to the use of Z76 material. Concurrent with this evaluation, surface modifiers should be studied to enable production of foam ceramics with the desired optical properties.
4. The use of a foam ceramic as a thermal insulation for aerospace vehicles, is contingent upon the mating of the foam to substrate materials. Accordingly, the adhesive properties and/or methods of anchoring the ceramic should be investigated.

REFERENCES

1. Petrocelli, A. W. and Kraus, D. L., "The Inorganic Superoxides", Journal of Chemical Education, Vol. 40, No. 3, March, 1963.
2. Petrocelli, A. W., "Development of Low Molecular Weight Compounds to Serve as Solid State Storage Media for Oxygen", General Dynamics Corporation/Electric Boat Division, U 413-62-070, February, 1962.
3. Blocker, E. W. et al, "Development and Evaluation of Insulating Type Ceramic Coatings", Marquardt Aircraft Co., WADC TR 59-102, November, 1959.
4. Kallup, C., Sklarew, S., and Castner, S. V., "Application and Evaluation of Reinforced Refractory Ceramic Coatings", the Marquardt Corporation, ML-TDR-64-81, June, 1964.
5. Edlin, V., "Interim Report on the Bonding Reaction Mechanism in Chemically Bonded ZrO₂ - Phase II", Douglas Aircraft, S14-45974, August, 1964.
6. Blocker, E. W. et al, "Reinforced, Refractory, Thermally Insulating Coatings", a paper presented at the SAE National Aerospace Meeting, Los Angeles, California, October, 1964.
7. Harrison, D. E., McKinstry, H. A. and Hummel, F. A., "High-Temperature Zirconium Phosphates", "Journal of the American Ceramic Society", Vol. 37, No. 6, June, 1954.
8. Weisert, E. D., "A Composite Materials System for Re-entry Vehicle Applications", The Marquardt Corporation, S-181, December, 1960.
9. Mine Safety Appliances Co., Callery, Pennsylvania, Private Communication, July, 1965.
10. Vukasovich, M. S. et al, "Foamed Ceramic", U.S. Patent No. 3,148,996, granted September, 1964.
11. Ozark-Mahoning Company, Tulsa, Oklahoma, Private Communication, February, 1966.



ZrO₂-H₂PO₃F reacted 30 minutes

ZrO₂-H₂PO₃F reacted 60 minutes

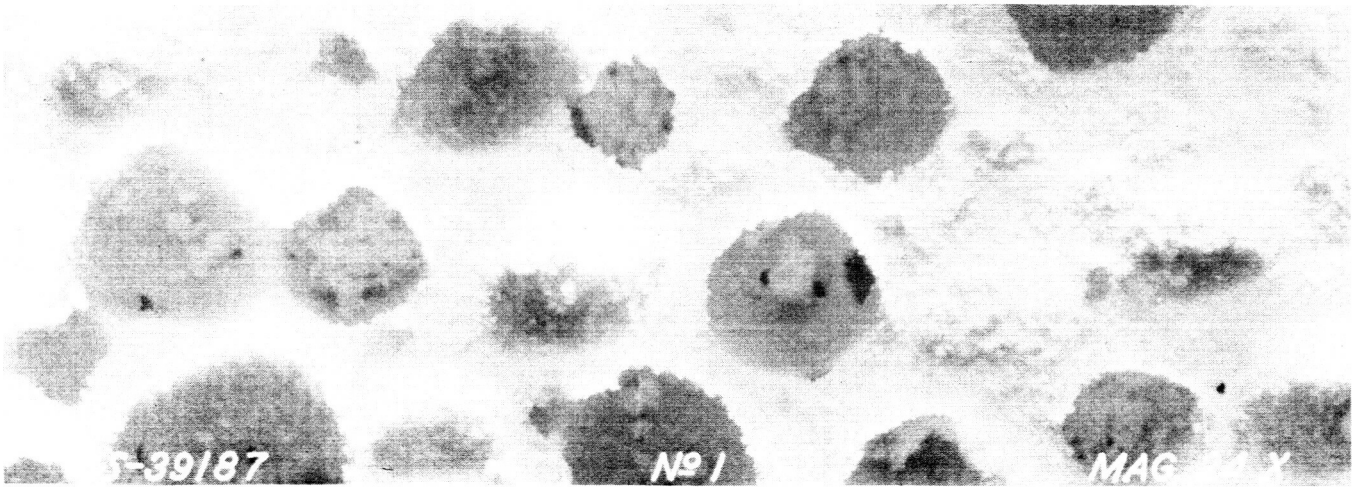
Figure 1. Comparison of Reaction Time Z76 Foam

S-39/79

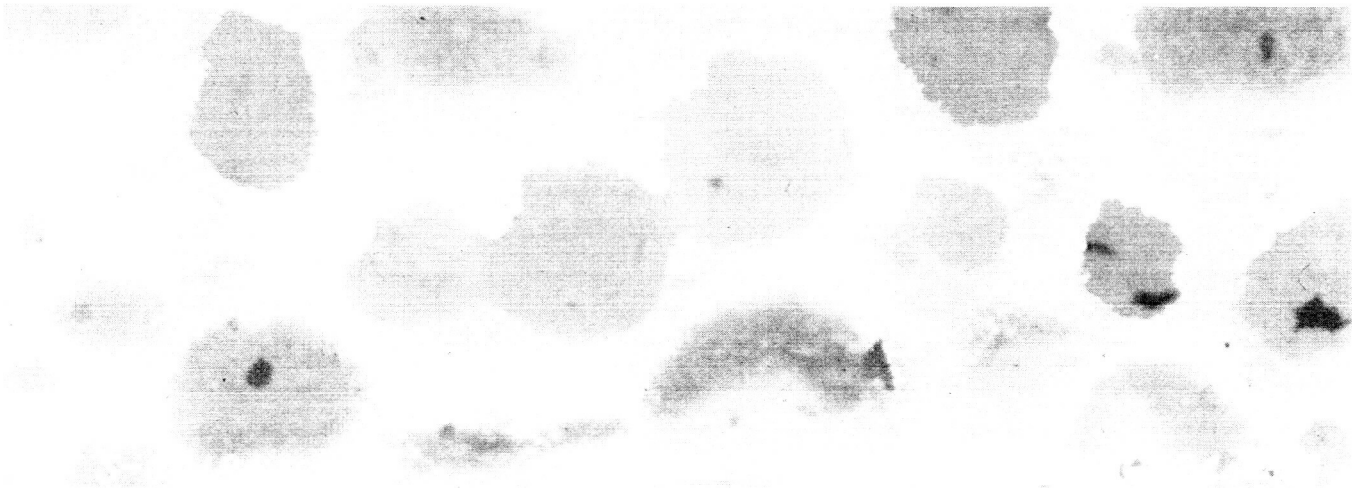


Figure 2. Foam Ceramic Body Showing Internal Structure

S-39/80



Pore structure at 0.25 inch rise

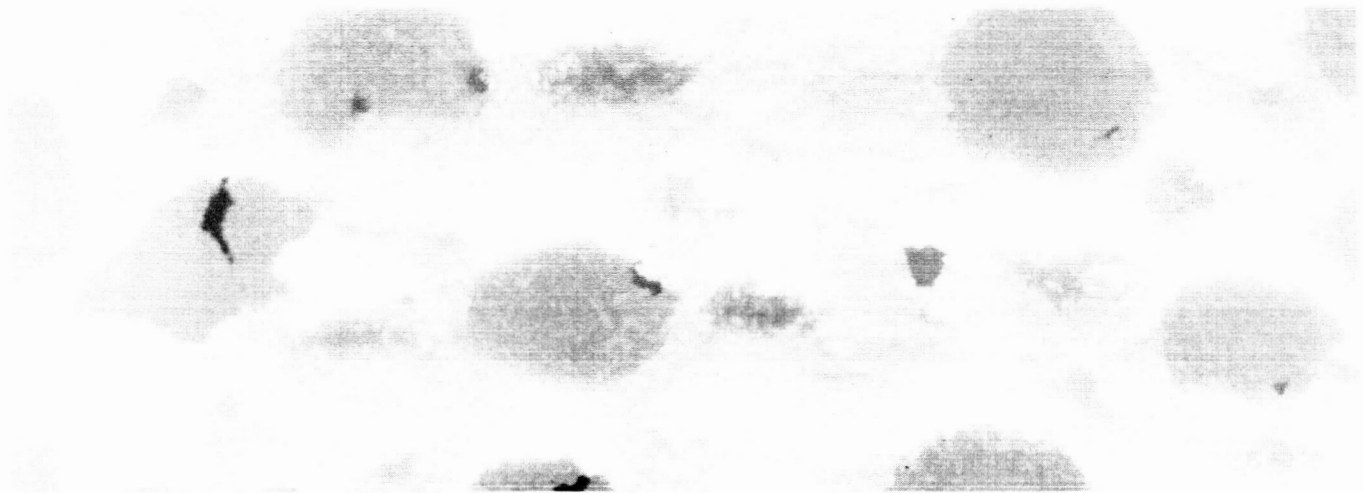


Pore structure at 0.50 inch rise



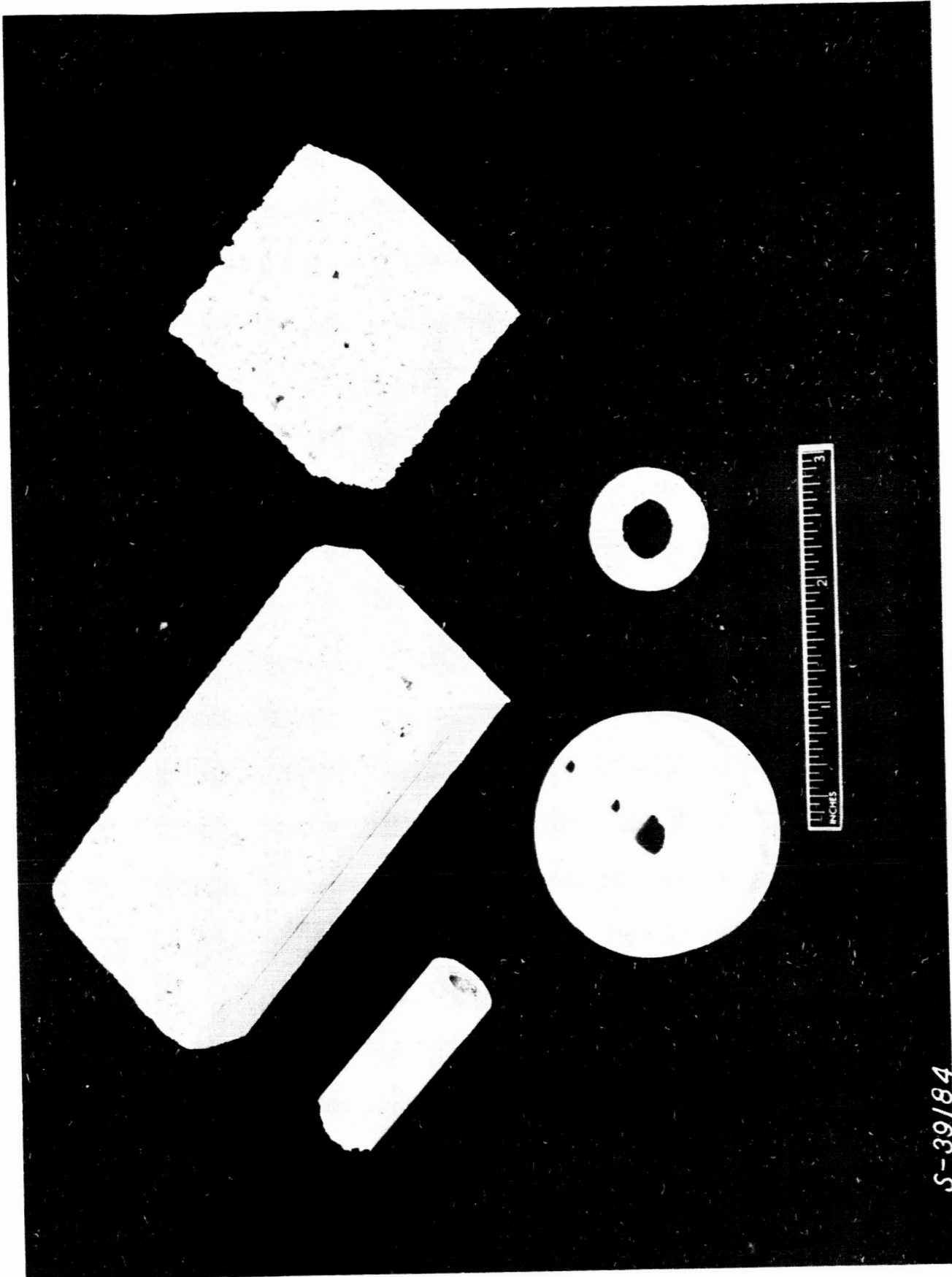
Pore structure at 0.75 inch rise

Figure 3. Photomicrograph of Z76 at Various Levels of Foam Rise



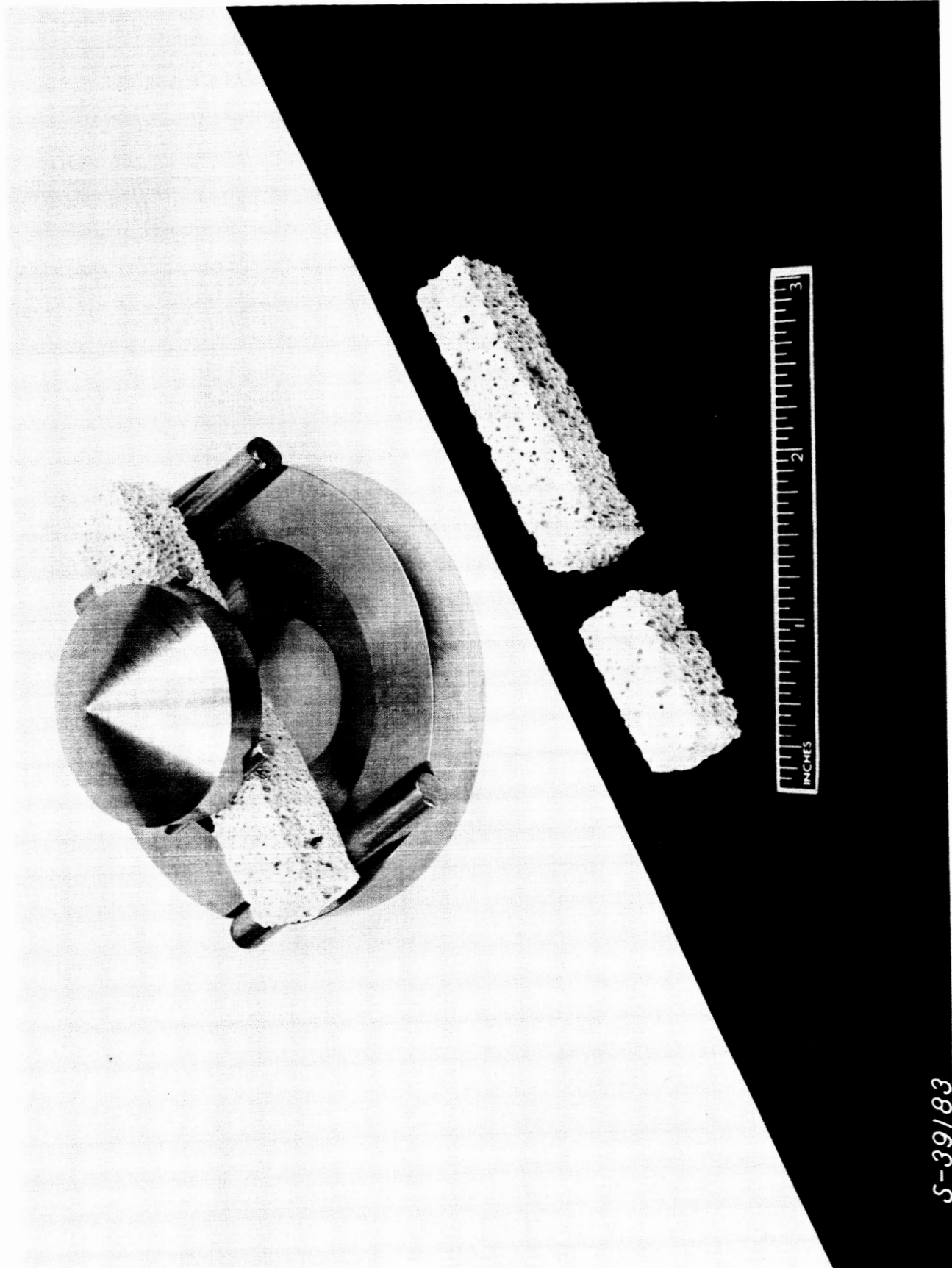
Direction of Rise

Figure 4. Photomicrograph of Z76 Foam Normal to Direction of Rise



S-39/84

Figure 5. Foam Ceramic Shapes



S-39/83

Figure 6. Modulus of Rupture Fixture

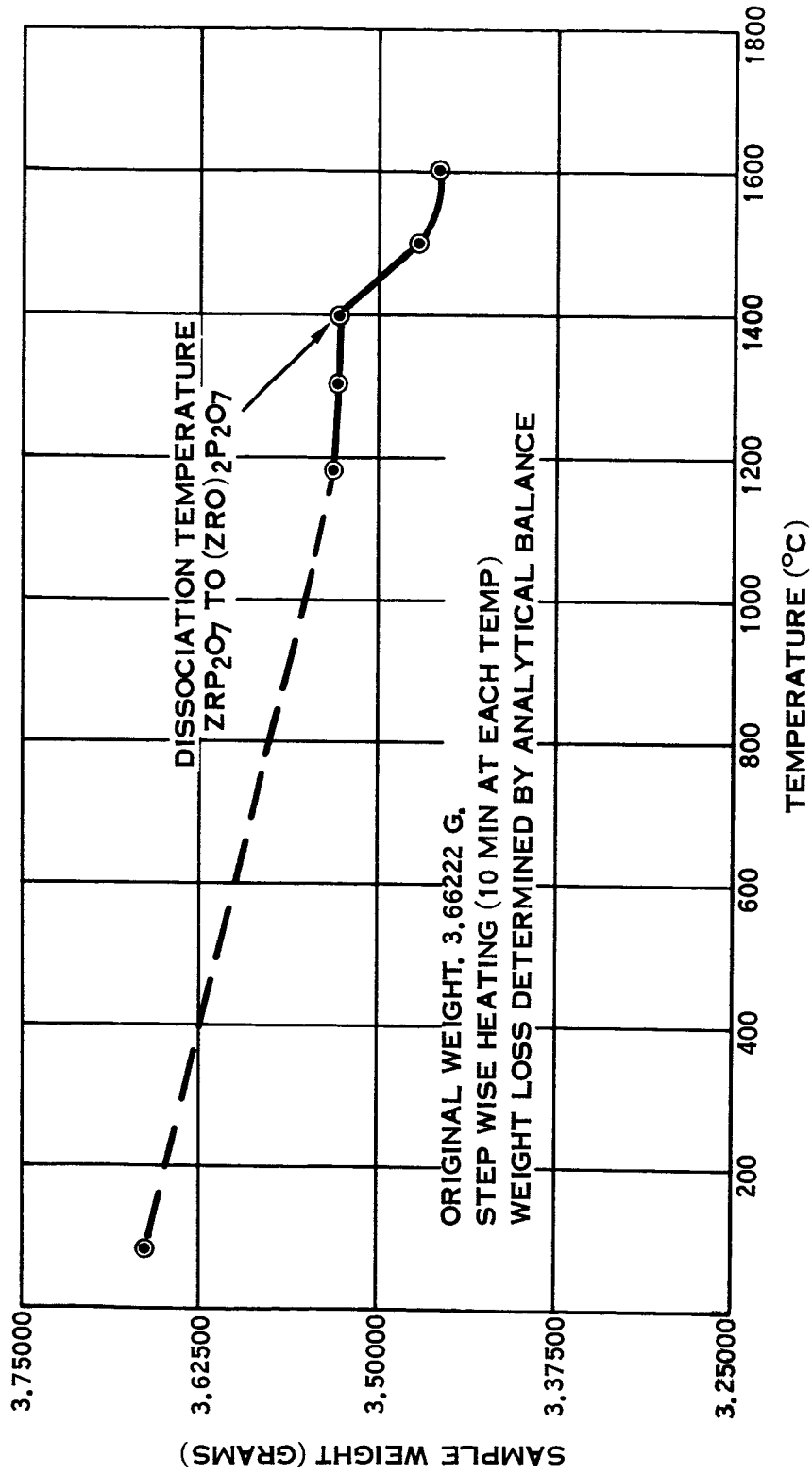


Figure 7. Thermal Stability Curve Z76 Foam

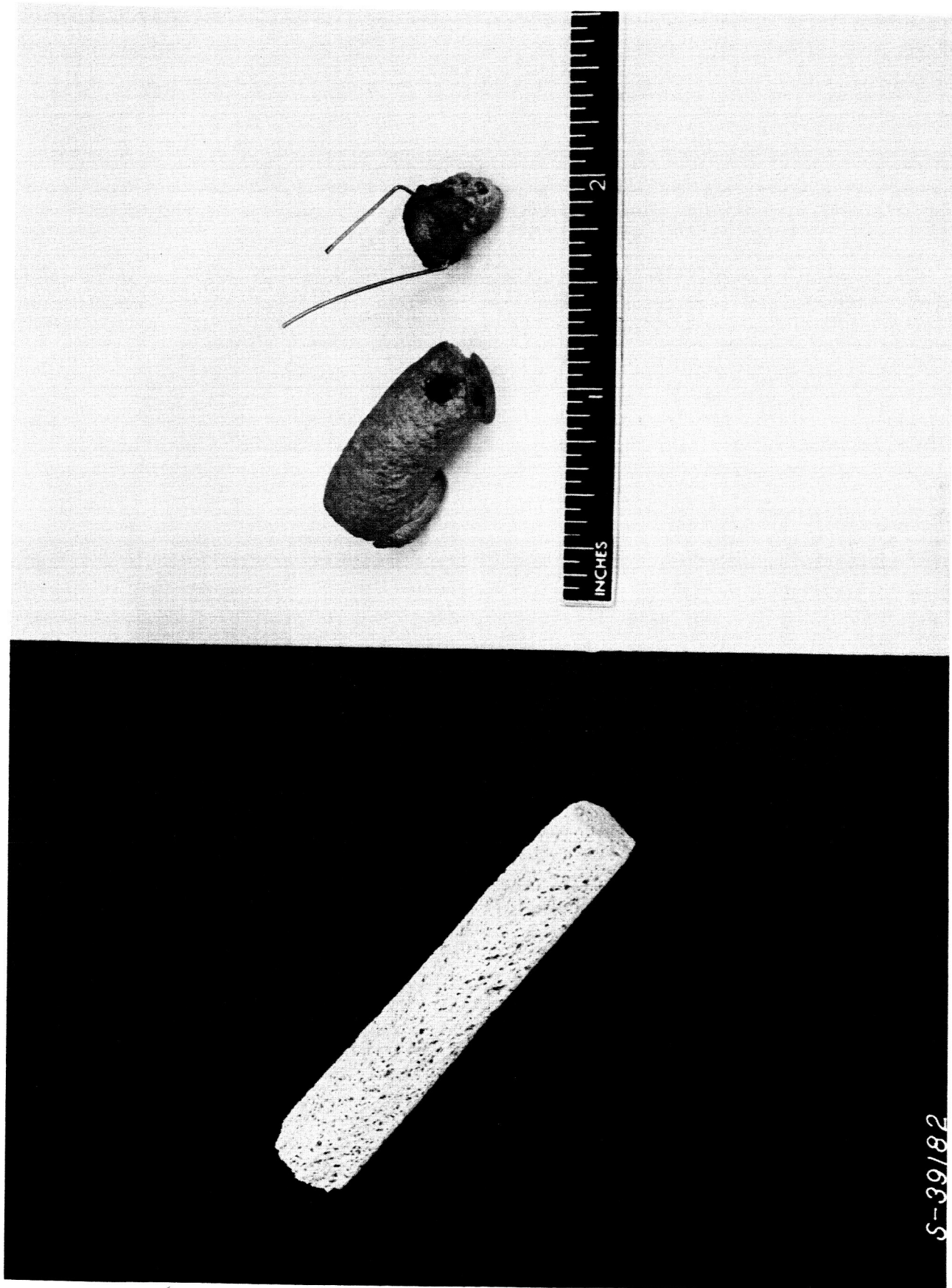
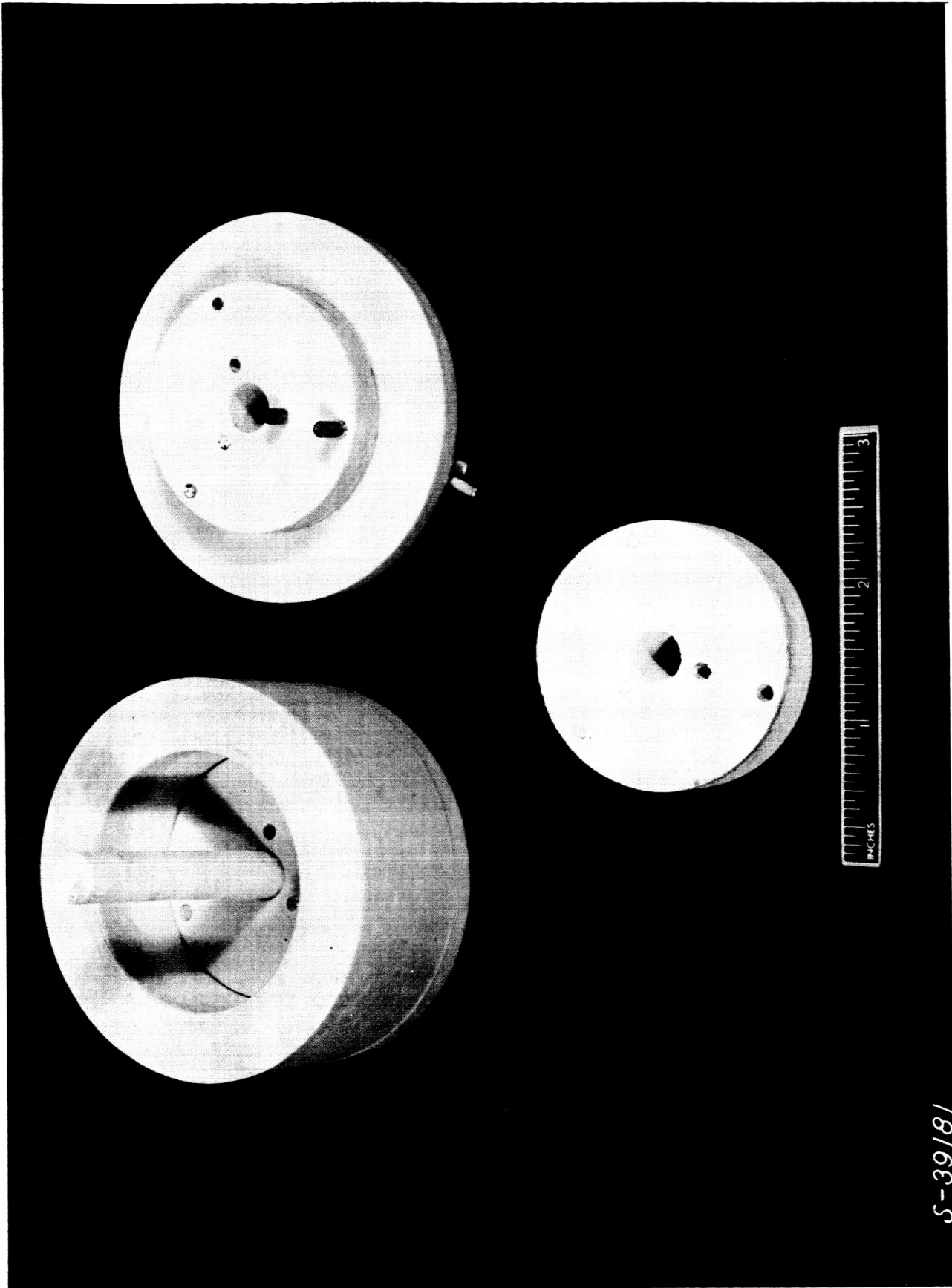


Figure 8. Z76 Melting Point Specimen



S-39/8/

Figure 9. Thermal Conductivity Details

APPENDIX A

TYPICAL PREPARATION OF Z76 FOAM BODY

The slurry preparation is accomplished by a stepwise addition of materials and mixing technique. The development of stoichiometric ratios can best be shown by a rearrangement of the Z76 formulae.

Z76

1) ZrO ₂	73.8 g.
2) NH ₄ H ₂ PO ₄	5.1 g.
3) AlOOH	4.0 g.
4) H ₂ PO ₃ F	120.0 g.
5) ZrO ₂	73.8 g.
6) NH ₄ H ₂ PO ₄	5.1 g.
7) Li ₂ O ₂	2.0 g.
8) Bentonite	2.0 g.

Item 1, 2, and 3 were blended intimately and charged into a polyethylene beaker immersed in a cold (45-60°F) water jacket. Acid (item 4) was added and mixed mechanically at a relatively slow speed. The mixing paddle was traversed periodically from the bottom to the top of the slurry volume. The mixing period has been established at 60-90 minutes. During this operation HF is liberated by chemical reaction and the evolution is manifested by the appearance of many small bubbles that burst at the slurry surface. This is characterized by the pungent odor of HF fumes. Completion of this mixing phase is indicated by the cessation of gas bubbles. The mixing action is never vigorous enough to entrain air in the slurry. The slurry at this point is a thin creamy fluid without entrained bubbles.

Items 5 and 6 are mixed intimately and added slowly to the slurry with constant mixing. This step provides excess ZrO₂ to assure reaction of all the H₂PO₃F, and develops the refractory characteristic of the foam body. A mixing time of 5-10 minutes is sufficient. The slurry is a heavy creamy fluid that appears bubble free.

The mixer speed is faster but does not whip the slurry during the addition of items 7 and 8. The Li₂O₂ is added and dispersed thoroughly during a 30-60 second mix. Bentonite is added immediately and the slurry is mixed for 60-120 seconds to effect disperment. At this point, bubble formation resulting from the Li₂O₂ reaction can be observed.

APPENDIX A (CONTINUED)

The slurry is charged into a suitable mold container and allowed to stand for periods of 10-30 minutes. Initiation of the foam rise is evident during this time. The mold is tightly capped and allowed to stand at room temperature for an additional time period. Experimental evidence indicates that a "rise" time of twelve hours is required to provide a fully blown ceramic foam that has developed into a plastic state. The mold and slurry are charged into a cold oven and brought to 300°F in a stepwise curing cycle. The absence of added water and the small volume of water released during reaction allowed the curing process to pass through the "water smoking" period rapidly. The prime consideration was the avoidance of the exothermic Li_2O_2 -water reaction. The long time room temperature cure minimizes this danger.

After a two hour cure at 300°F, the foam ceramic has developed a hard body and may be handled. In the event water solubility is not a problem the foam body is now ready for use. To insolubilize the foam ceramic body, a further cure of four hours at 500°F is required.

APPENDIX B

GLOSSARY OF MATERIALS

Material	Source	Data Screen Analysis
1. Alkaphos CE $Al_2O_3 \cdot 3P_2O_5 \cdot X H_2O$	Monsanto Chemical Co.	Viscosity at 25°C 500- 2000 centipoise
2. Alumina T61 Al_2O_3 tabular	Aluminum Co. of America	-325 mesh 100%
3. Aluminum #101 Aluminum metal powder	Aluminum Co. of America	-100 mesh 100% -325 mesh 80% ave. dia. 19-20 microns
4. Ammonium dihydrogen phosphate $NH_4H_2PO_4$	Matheson Coleman & Bell	
5. Bentonite	Chicago Vitreous Corpora- tion	
6. Baymal colloidal alumina ALOOH	E.I. DuPont de Nemours & Co.	Specific surface area 274 m ² /g
7. Calcium carbonate $CaCO_3$	Fisher Scientific Co.	
8. Calcium silicate $CaO \cdot SiO_2$	Hampden Color & Chemical	Micron sized powder
9. Fluophosphoric acid, mono H_2PO_3F	Ozark Mahoning	Anhydrous 80% H_2PO_3F
10. Hydrogen peroxide H_2O_2	Fisher Scientific Co.	
11. Kasil #6 Potassium silicate	Philadelphia Quartz Co.	$K_2O:SiO_2$ ratio 1:2.10 40.3° Be
12. Lithium peroxide Li_2O_2	Foote Mineral Company	Ground to 100%-35 mesh
13. Phosphoric acid H_3PO_4	Mallinckrodt Chemical Co.	85%

APPENDIX B (CONTINUED)

Material	Source	Data Screen Analysis
14. Phosphorus pentoxide P_2O_5	Matheson, Coleman & Bell	
15. Potassium super oxide KO_2	MSA Research Corp.	16-20 mesh 100% O_2 content 223 cc/g
16. Potassium permanga- nate	Fisher Scientific Co.	
17. Silica Cab-O-sil SiO_2 micron size	The Cabot Corporation	
18. Corn Starch		
19. Zirconia Zircoa B ZrO_2	Zirconium Corp. of America	CaO stabilized, partially fused, 100%-325 mesh
20. Wetting Agent Triton X100	Rohm and Haas	
21. Wollastonite $CaO \cdot SiO_2$	The Cabot Corporation	C101 granular

APPENDIX C

THERMAL PROPERTIES OF ALKALI METAL PEROXIDE AND
SUPEROXIDE BLOWN CERAMIC FOAM Z76
(UNITED AIRCRAFT RESEARCH LABORATORIES)

In accordance with purchase order HSD-574363, July 19, 1965, the experimental and analytical work necessary to establish the thermal conductivity, the thermal gravimetric, and the melting point properties of zirconia foam Z76 have been carried out and are here reported.

The weight loss of this material as a function of temperature was determined by heating a finely ground portion of sample Z76 in a beryllia crucible by means of a high-temperature ceramic kiln operated in air. The sample was heated to the temperature specified in the table below and then held at that temperature for 10 minutes, removed from the kiln and allowed to cool and then weighed on a Mettler single-pan balance with the results shown.

Temperature		Sample Weight (grams)
°C	°F	
27	80	3.66222
1180	2156	3.53130
1300	2372	3.52668
1400	2552	3.52584
1500	2732	3.47330
1600	2912	3.45920
1650	3002	3.36922*

* BeO crucible collapsed. This value may, therefore, be too low.

When examined at the final temperature obtainable in this kiln, 1650 C or 3002 F, the sample had not melted but had sintered to a solid mass.

To determine the melting point of the material, Z76, a rod of the sample 1 1/2 in. long and 1/2 in. in diameter was first drilled transversely near one end, preheated to 1000 C for two hours in air, then cooled and hung by means of a tantalum wire in the tungsten resistance furnace of Figure 1. This furnace was then pumped down, flushed with argon, and finally filled with argon at a pressure of 4 1/2 psi over atmospheric. The sample was then heated until melted, the temperature being determined by reading with a "Pyro" micro-optical pyrometer the temperature of the inside of a tungsten crucible in which the specimen is hung. The sample melted at an observed optical temperature, 1762 C, which through the use of the calibration curve shown in Figure 2 may be converted to a true temperature of 1835 C + 10 C (i.e. approximately 3335 F). The melting point at zirconia foam Z76 is therefore 1835 C in an argon atmosphere 4.5 psi above atmospheric pressure.

The thermal conductivity of the zirconia foam material was measured by a method yielding a relatively close approach to the idealized concept of radial heat flow without an appreciable longitudinal heat flow component and which consists

of approximating the "infinite" length through the use of a stack of thin discs, all of the same material. The longitudinal heat flow is limited by the poor thermal contact between adjacent discs so that essentially true radial flow exists over a finite length near the longitudinal center of the stack. An indication of the magnitude of the longitudinal heat flow can be obtained in the test by measuring the longitudinal temperature profile with a thermocouple placed at a given radial position and then moved through the range in height of interest.

This technique has been used by several investigators. Fieldhouse, et al (Ref. 1) used a stack of discs with a height to diameter ratio of 2.0 to 1, end-guard heaters with approximately the same temperature profile as the specimen to limit longitudinal heat flow, a central heater to provide the thermal gradient, and an external heater to raise the temperature of the system. Feith (Refs. 2, 3) in measuring the thermal conductivity of beryllia foam specimens dispensed with the end-guard heaters by using a stack of discs having a height to diameter ratio of a little greater than two (2.25 to 2.75), placing the stack in a refractory metal crucible in an attempt to further equalize temperature differences, and placing a stack of radiation heat shields on top of the stack of discs to further reduce axial heat flow. Like Fieldhouse (Ref. 1), Feith (Refs. 2, 3) used a central heater to create the desired thermal gradient and an external heater to raise the temperature of the system.

The UACRL stacked-disc radial heat flow apparatus is based on Feith's work (Refs. 2, 3) with a few simple improvements as shown schematically in Figure 3. The UACRL tungsten resistance furnace, which provides the long isothermal heat zone essential for thermal conductivity measurements, has been used to house the experiment. In the furnace, a vertical stack of seven discs of the material, whose thermal conductivity is to be studied, is placed in a deep thin-walled tungsten crucible and a thin disc of tungsten is placed on top of the stack of discs in an attempt to form an isothermal shell. An additional source of heat, which is constructed from 20 mil wall tantalum tubing, is inserted on the axis of the tungsten crucible, tungsten lid, a stack of discs and is mechanically supported by a dead-end hole in a boron nitride plug inserted in the lower water-cooled copper electrode and aligned by a centering hole in a massive boron nitride disc placed in the upper water-cooled copper electrode of UACRL tungsten furnace. The tungsten furnace is then used to heat the sample to the temperature at which the thermal conductivity measurement is made and the inner tantalum tube is used to produce a radial temperature gradient across the stack of discs at this temperature. Temperatures are read exclusively with platinum-platinum, 10% rhodium thermocouples. The furnace elements, specimen and crucible, and tantalum heater tube are protected by evacuating the furnace to 1×10^{-6} mm of Hg and then flowing purified argon through the furnace at a controlled rate such that a constant positive pressure of 4.5 lbs/in.² is maintained.

The UACRL tungsten furnace shown schematically in Figure 3 has been described in detail in earlier publications (Ref. 4). Very briefly, the furnace uses flat sheets of either 5 mil tungsten or 7 mil tantalum arranged to form a rectangular box 10 in. long x 3 1/2 in. x 3 1/2 in. and so offers an unusually long and large isothermal central section approximately 3 1/2 in. long and 2 1/2 in. in diameter.

The heating elements are surrounded on all sides by 8 sets of tantalum radiation shields, a mirror finish stainless steel reflecting shell and a water-cooled jacket to further assure constant temperature. The vacuum system comprises a 6 in. diffusion pump, 6 in. valve with water-cooled baffle, and a liquid nitrogen trap and is capable of achieving a vacuum of 1×10^{-7} mm Hg with cold furnace, and typically a vacuum of 3×10^{-5} mm Hg at a temperature of 2500 C. The furnace temperature range is 100 C to 2800 C and constant temperatures of 2500 C may be achieved in four minutes (without sample) since there are no ceramic materials in the furnace.

The insert tantalum tube heater consists of a 20 mil, 1/4 in. diameter eleven-inch long tantalum tube with that two-inch portion of the tube centrally located in the specimen stack reduced to 15 mil thickness to minimize end effects. The heating current is introduced in the tantalum tube by pressed molybdenum sheet contacts which are joined to solid 1/8 in. molybdenum rod electrodes. The molybdenum rods leave the furnace through Conax fittings as vacuum seals. Two voltage leads are attached to the tantalum heater tube at the ends of the centrally thinned section. The current supplied to the insert tantalum tube heater is measured by means of a thermocouple ammeter and a calibrated current transformer, while the voltage drop across that portion of the tantalum tube heater reduced in thickness from 20 to 15 mils is measured by a true r.m.s. electronic voltmeter attached to the 20 mil diameter molybdenum voltage leads. The product of the current and voltage readings divided by the distance between the voltage leads is used to calculate that heat flow in watts/cm which causes the desired radial temperature differential. In the actual experiment, the current input to the tantalum insert heater is held at 100 amperes much of the time and typical potential differences of 0.100 to 0.700 volts result when an effort is made to maintain a radial temperature difference of approximately 100 C across the specimen. A 100 C or greater radial temperature differential serves to minimize any errors resulting from the longitudinal (axial) temperature differences present in the experiment.

As indicated schematically in Figure 3, temperature are read by means of thermocouples at six positions in the stacked-disc sample. The details of the specimen construction are shown in Figure 4, where it can be seen that two temperatures are read at radial distances of 0.686 in. and 1.686 in. on a given radius in the third disc of the specimen, at the same radial distances but on a radius rotated 120 in the fourth disc of the specimen, and again at the same radial distances but on a radius 240° away in the fifth disc. The top and bottom pairs of discs in the seven-disc stack serve only as guard specimens and are not instrumented. Because of the high target temperature of the experiment (2200 C), all thermocouples used are platinum vs platinum 10% rhodium and are protected both by using double-bore beryllia thermocouple tubing and by flame-spraying the thermocouple bead with zirconia.

TEST PROCEDURE FOR RADIAL HEAT FLOW STACKED-DISC METHOD

In general, the procedure consisted of setting the power level of the tungsten furnace at a given level and then taking continuous temperature readings on all six thermocouples until the temperature readings at the lower four locations agreed within ± 2 C and did not change more than 1 C in a five-minute period. The center heater was then turned on and the power adjusted to obtain a thermal gradient of approximately 100 C. The system was assumed to be in a steady-state condition when the temperature gradients in the two planes agreed within ± 2 C and did not change more than 0.1 C in a five-minute period. After completing observations at one temperature, the external system temperature was raised approximately 100 C and the procedures outlined above were then repeated at this new temperature. The temperature measurements from room temperature to approximately 1500 C were made with platinum-platinum, 10% rhodium thermocouples.

The measured values of the thermal conductivity for zirconia foam Z76 are shown in tabular form below and graphically in Figure 5. The reproducibility of such measurements have been shown to be very high in this laboratory (Ref. 5), but the absolute value is dependent on the machining characteristics of the material tested, i.e. on the accuracy of the spacing of the thermocouple wells. Typically, measurements are expected to be reproducible to within $\pm 1/2$ of 1% and correct to within $\pm 10\%$.

TABLE I

APPARENT THERMAL CONDUCTIVITY, ZIRCONIA FOAM Z76

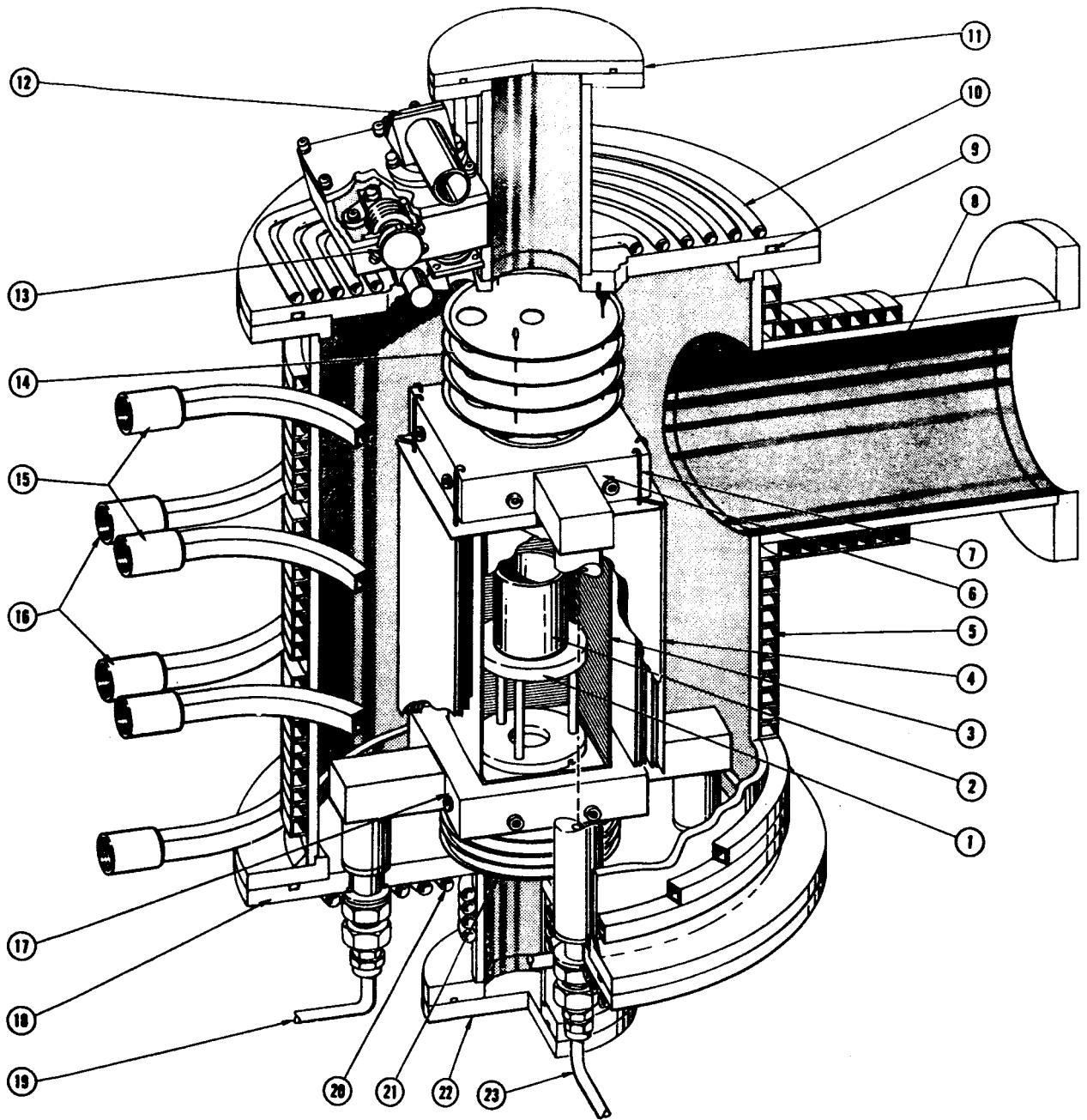
Mean Temperature		Thermal Conductivity (calories/sec °C-cm/cm ²)
°C	°F	
303.7	578.7	0.00112
466.6	871.9	0.00116
575.6	1068.1	0.00130
673.5	1244.3	0.00140
762.2	1404.0	0.00146
829.3	1524.7	0.00147
845.3	1553.5	0.00155

The graph of the thermal conductivity of zirconia foam, Z76, shown in Figure 5 shows a lower or improved value of thermal conductivity when compared to the four commercially available zirconia foams previously tested in this laboratory (Ref. 5).

REFERENCES

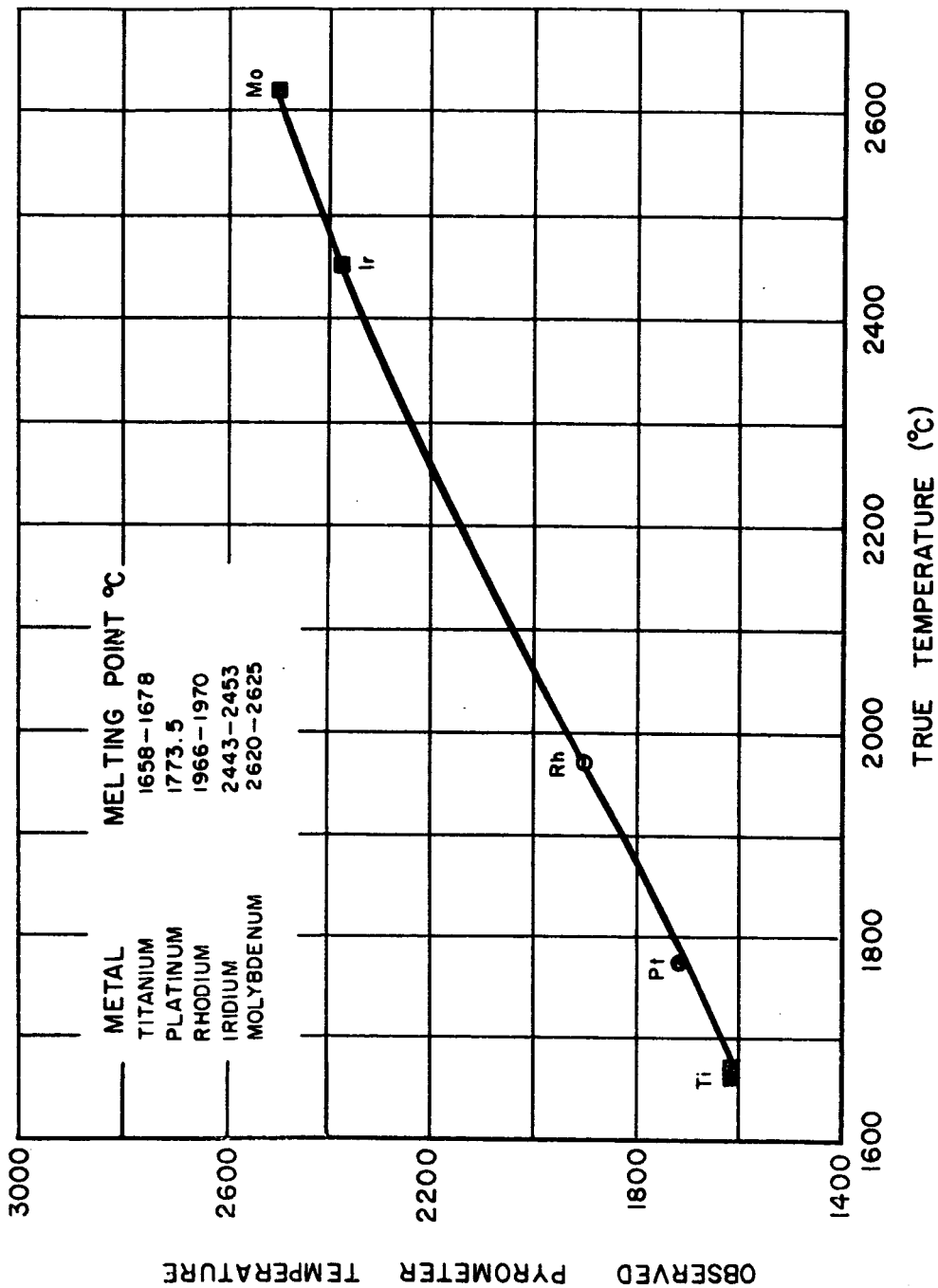
1. Fieldhouse, I. B., and J. C. Hedge: Measurements of Thermal Conductivity of Uranium Oxide. AEC U3381, September, 1956, p. 2.
2. Feith, A. D.: Thermal Conductivity of UO_2 by a Radial Heat Flow Method. Third Conference on Thermal Conductivity, Gatlinburg, Tennessee, October 16-18, 1963, pp. 162-180.
3. General Electric Co., Nuclear Materials and Propulsion Operation High-Temperature Materials Program, Progress Report No. 9, Part A, March 30, 1962, Section 7 High Temperature Insulation Materials (57010), pp. 67-70.
4. Bacon, J. F., R. D. Veltri, and J. Y. Whittier: High Temperature Vacuum Furnace with Metallic Sheet Resistance Elements. Rev. Sci. Instr., Vol. 34, No. 11, November, 1963, pp. 1200-1201.
5. Bacon, J. F.: The Evaluation of Foam Ceramics for Application to Advanced Power Plants. Second Interim Progress Report No. 2 - June 1, 1964 to September 1, 1964, UAC Research Laboratories Report UAR-C148, issued October 23, 1964.

HIGH TEMPERATURE TUNGSTEN RESISTANCE FURNACE

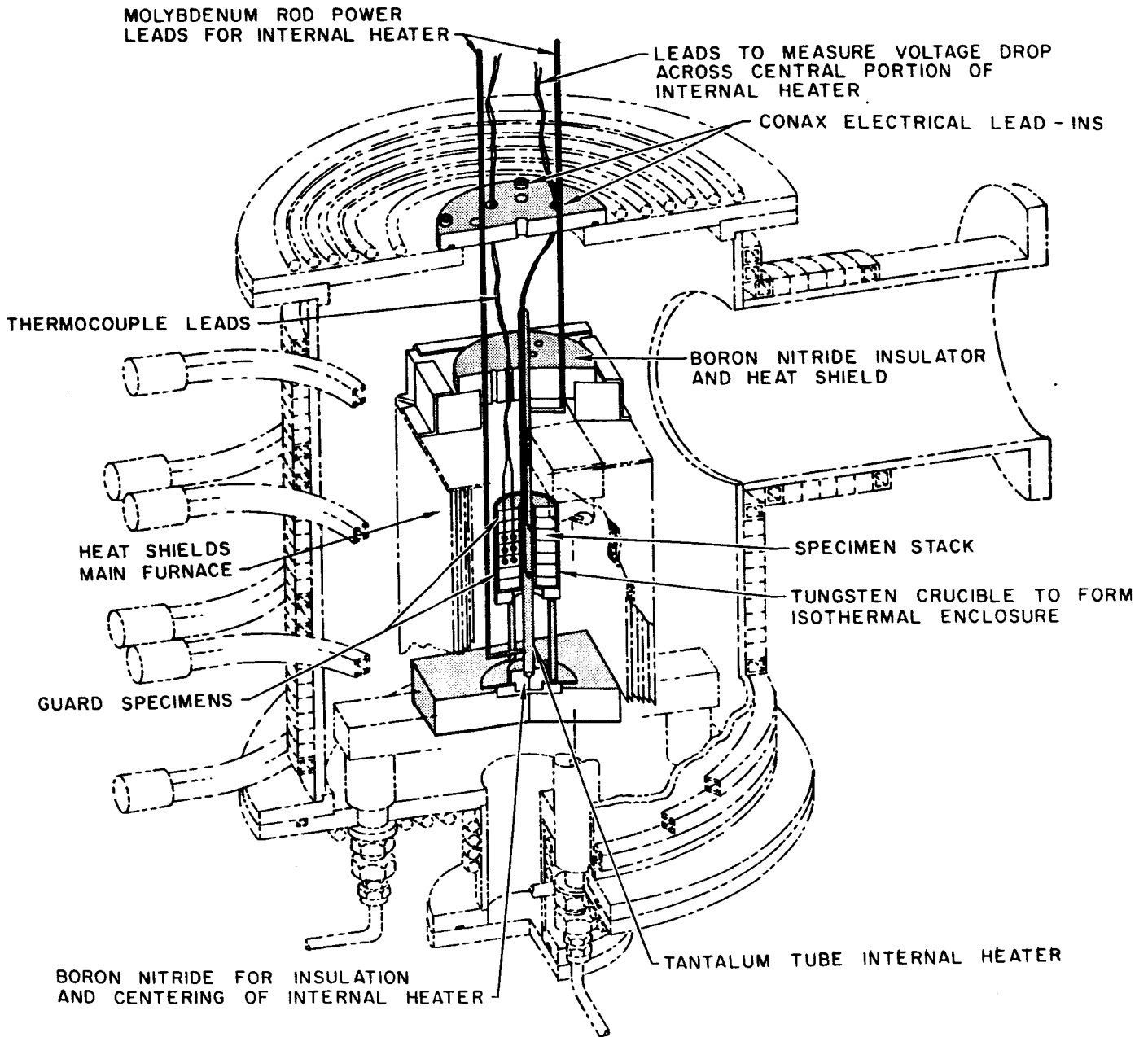


- | | |
|--|---|
| ① TUNGSTEN PEDESTAL FOR CRUCIBLE | ⑬ PROTECTOR MECHANISM FOR SIGHT GLASS |
| ② TUNGSTEN CRUCIBLE | ⑭ TOP TANTALUM RADIATION SHIELDS |
| ③ FLAT TUNGSTEN HEATING ELEMENT (4) | ⑮ COOLING WATER IN |
| ④ TANTALUM RADIATION SHIELDS | ⑯ COOLING WATER OUT |
| ⑤ SIDE COPPER COOLING COILS | ⑰ BOTTOM WATER COOLED ELECTRODE SUPPORT CONDUCTOR |
| ⑥ TOP WATER COOLED ELECTRODE SUPPORT CONDUCTOR | ⑱ BOTTOM PLATE FOR MOUNTING |
| ⑦ SUPPORT PIN FOR TANTALUM SHIELDS | ⑲ WATER IN BOTTOM ELECTRODE |
| ⑧ TO VACUUM SYSTEM | ⑳ BOTTOM COPPER COOLING COILS |
| ⑨ "O" RING GASKET SEALS | ㉑ BOTTOM TANTALUM RADIATION SHIELDS |
| ⑩ TOP COPPER COOLING COILS | ㉒ BOTTOM INTERCHANGABLE COVER FOR MEASURING APPARATUS |
| ⑪ TOP INTERCHANGABLE COVER FOR MEASURING APPARATUS | ㉓ WATER IN TOP ELECTRODE |
| ⑫ SIGHT GLASS | |

PYROMETER CORRECTION CURVE

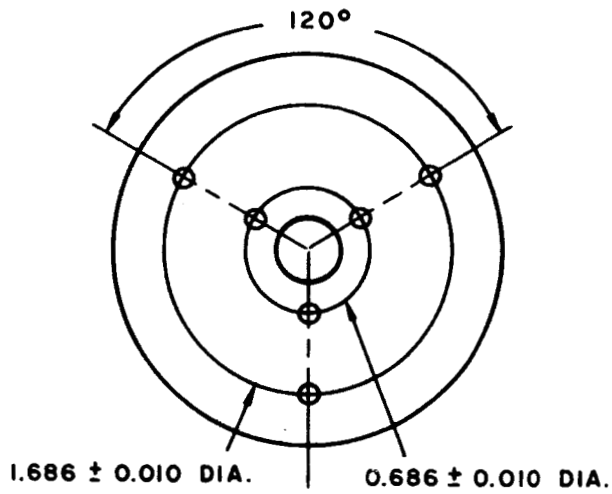


ARRANGEMENT OF APPARATUS IN TUNGSTEN FURNACE FOR STACKED-DISC RADIAL HEAT FLOW THERMAL CONDUCTIVITY MEASUREMENTS

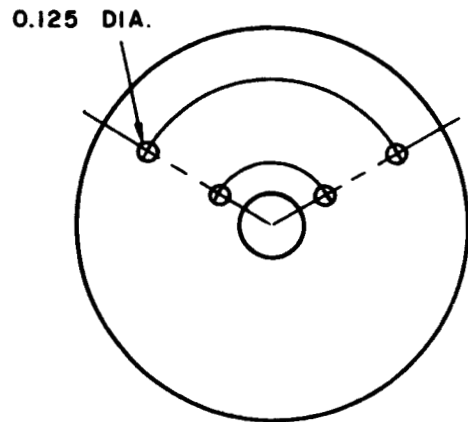


DESIGN OF THERMAL CONDUCTIVITY SPECIMENS

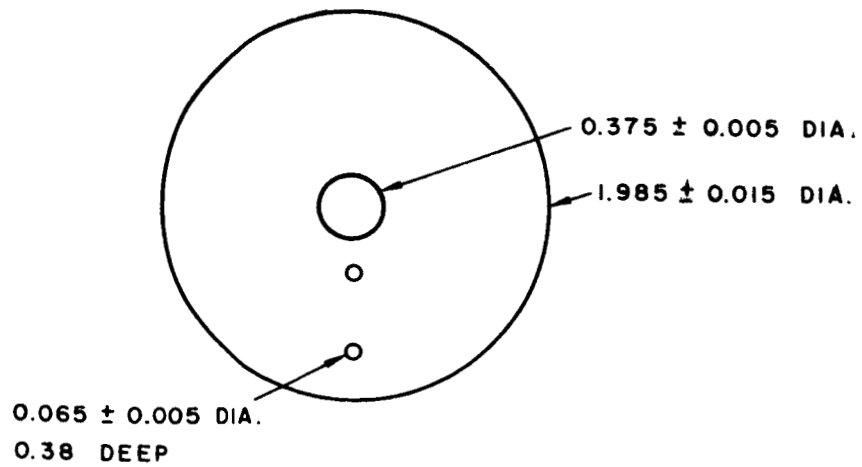
ALL DIMENSIONS
IN INCHES



UPPER GUARD

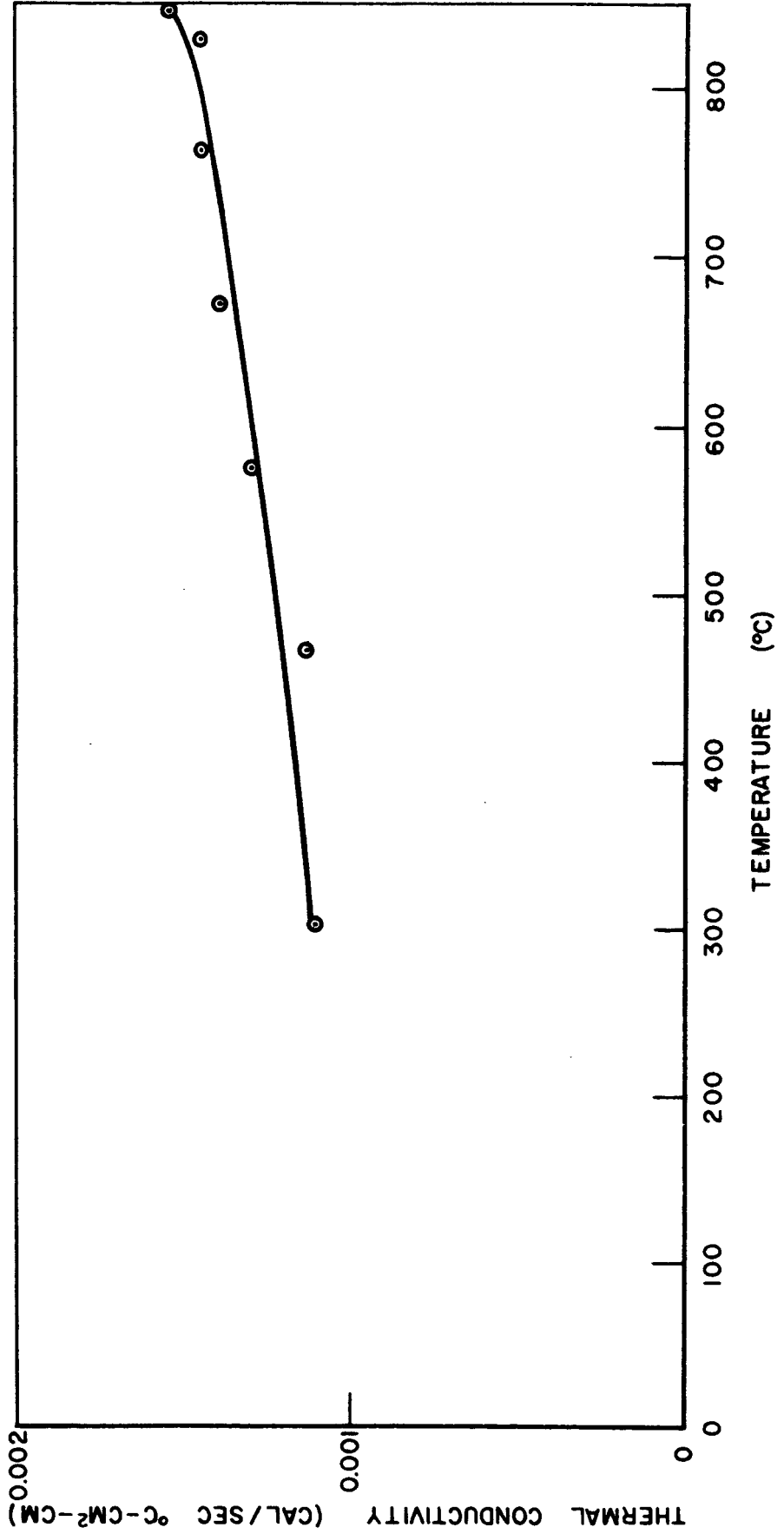


SPECIMEN



LOWER GUARD

APPARENT THERMAL CONDUCTIVITY
ZIRCONIA FOAM SAMPLE Z - 76
MEASURED UNDER 415 LBS/IN.² ARGON PRESSURE



APPENDIX D

OPTICAL PROPERTIES OF ALKALI METAL PEROXIDE
AND SUPEROXIDE BLOWN CERAMIC FOAM Z76
(PRATT & WHITNEY AIRCRAFT)

Introduction

A purchase order was received from Hamilton Standard Division requesting the measurement of total hemispherical emittance at temperatures above 500°F for foam ceramic samples. The samples were provided by Hamilton Standard Division.

The total hemispherical emittance of two samples was measured, but at temperatures below 500°F. The emittance values measured were 0.75 at 151°F and 0.78 at 317°F for two different specimens respectively.

Total Hemispherical Emittance Measurements

Test Procedure and Results

The total hemispherical emittance of two samples was measured in the total hemispherical emittance rig shown in Figure 1. The emittance was determined by electrically heating the specimens in vacuum and establishing a steady-state heat balance. A vacuum of 10^{-5} mm Hg or better was maintained to ensure that the effects of residual gas conduction and convection would be negligible. Hence, except for heat lost through thermocouple and power leads, all heat lost through thermocouple and power leads, all heat supplied to the specimen is lost by radiation. The inside wall of the vacuum chamber simulates a black body and is maintained at a constant, uniform temperature. This permits the Stefan-Boltzmann law to be used to calculate total hemispherical emittance from the measured quantities of the power supplied to the specimen, specimen surface temperature, and chamber wall temperature.

With this method of measuring total hemispherical emittance it was expected that best results would be obtained with tubular specimens. The proposed specimen configuration for total hemispherical emittance measurement is shown in Figure 2. Unfortunately, it was not possible to fabricate specimens to the desired configuration. Consequently, an attempt was made to obtain the required data with flat specimens. Two different specimens of this type were used. However, the use of these specimens limited both the accuracy of the results and the temperature range over which measurements could be made.

The first specimen consisted of a thin-film heating element sandwiched between two pieces of the foam ceramic material (see Figure 3). Ren epoxy was used to bond the layers together and to provide a uniform heat conduction path between the heater and the ceramic. The heating element consisted of a 1-mil thick Mylar film coated with a 0.002-mil thick layer of gold. The ceramic pieces measured 2 inches by 2 inches by 1/8 inch.

Power was supplied to the specimen by two 8.3-mil diameter copper leads soldered to the gold coating. These leads also supported the specimen in the vacuum chamber. The use of a single pair of leads, to supply both power and support the specimen, minimized thermal conduction losses.

The specimen was instrumented with two 0.003-inch diameter Chromel-Alumel thermocouples located at the center of each of the specimen faces. The thermocouples were attached to the surfaces with Sauereisen cement in a manner producing a minimum disturbance to the surface characteristics.

The specimen was heated in vacuum until thermal equilibrium was obtained at a temperature of 151°F. The data obtained at these conditions indicated an emittance of 0.75. The power to the specimen was then increased to provide data at a higher temperature, but the heating element failed, and the test was terminated.

To obtain data at a higher temperature, a second specimen was prepared to the configuration shown in Figure 4. This specimen incorporated a stainless steel heater to provide a higher temperature capability and dummy ceramic blocks at both ends of the test section to provide more uniform temperatures in the test section. In addition, the sample was bonded together with Sauereisen cement, which was better high-temperature characteristics than epoxy. Because of the high current required by the stainless steel heater, small diameter heater leads were not suitable. Water-cooled copper leads were therefore used. Heat conduction losses from the specimen through the leads were determined by measuring the temperature gradient along the leads with five thermocouples. Other instrumentation is shown on Figure 4.

The specimen was heated until equilibrium was established at a temperature of 317°F. The data was corrected for thermal conduction losses, and the resulting emittance value was 0.78. An attempt was made to obtain data at 390°F. At this temperature, however, the specimen surface temperatures were far from uniform, indicating partial separation of the ceramic from the heater. It was not possible to calculate an emittance value from the available data. No additional testing was attempted.

Discussion of Results

The error analysis indicates that lead losses and errors in thermocouple output, power, and specimen radiating area measurements contribute a total error of +4 per cent rms for the first specimen and +6 per cent rms for the second specimen. However, the total hemispherical emittance values presented are based on the assumption that the surface temperature measured represents the effective temperature of all areas of the specimen surface. Because of the specimen configurations used, and non-uniform porous surface structure, the surface temperature probably was not uniform, hence additional errors are probably present in the results. The magnitude of these errors cannot be determined accurately, but is believed to be significant. Emittance is also a function of the surface roughness and this factor varied considerably on the samples tested. It is recommended, therefore that the data presented herein be applied with discretion.

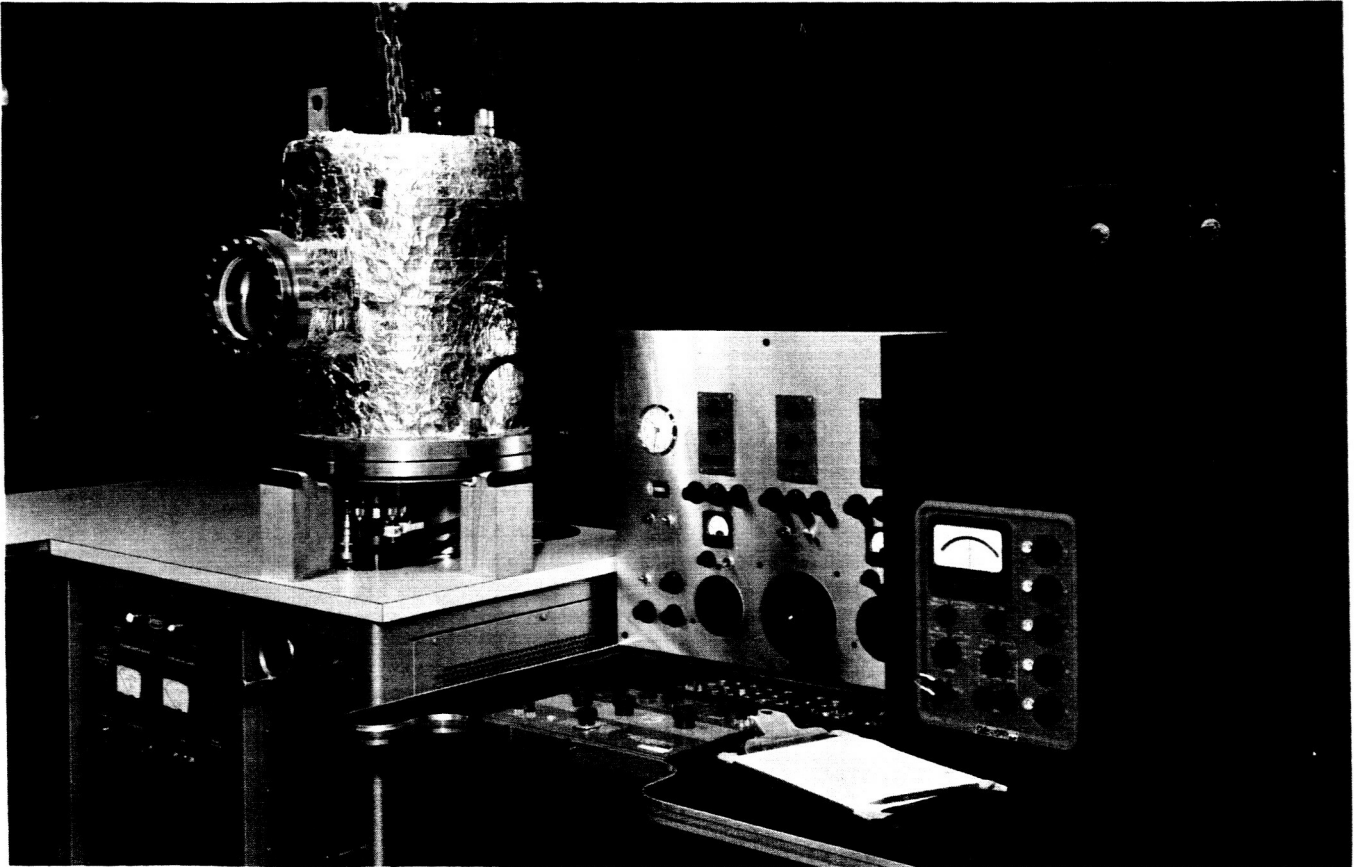


Figure 1. Total Hemispherical Emittance Rig

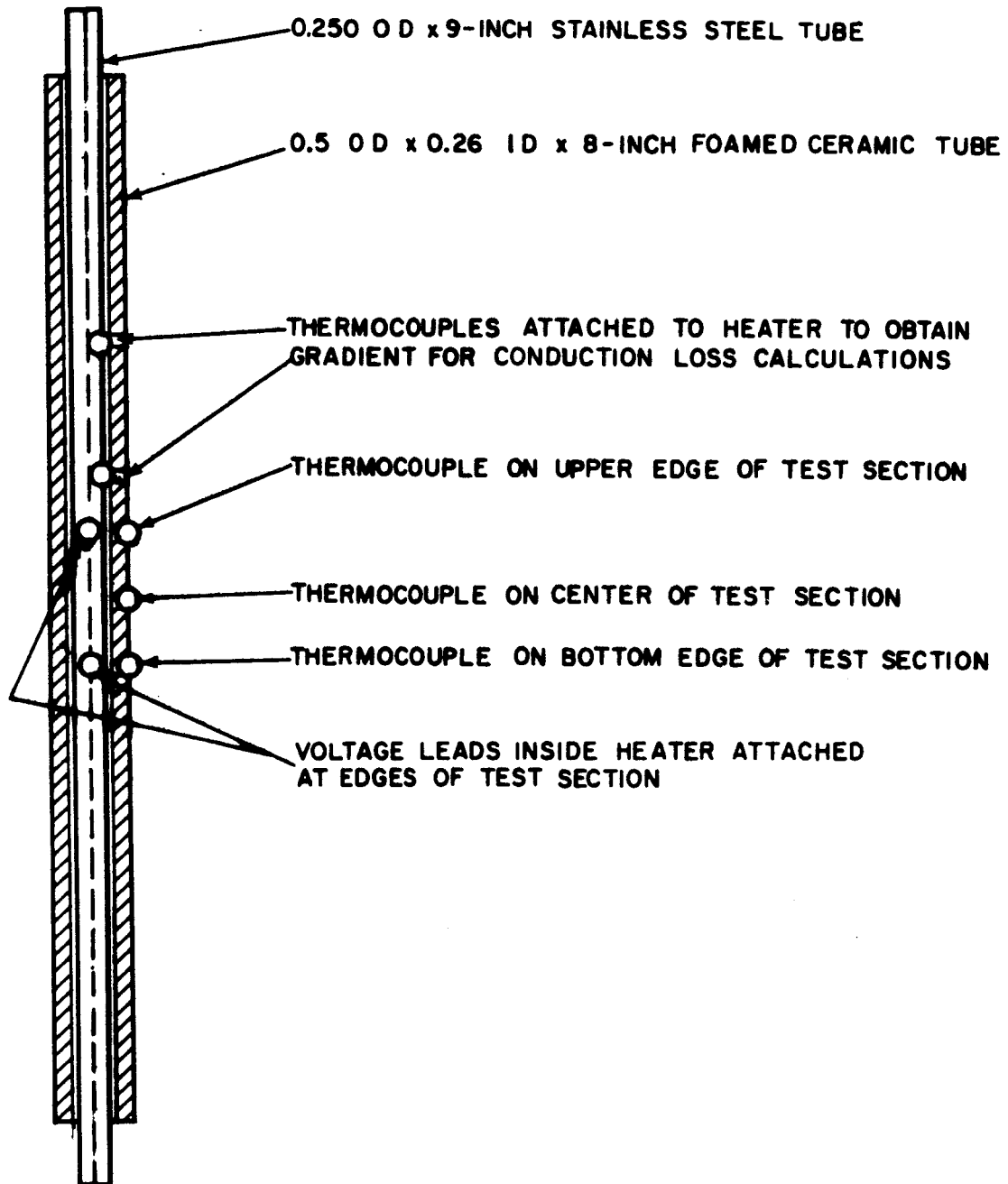


Figure 2. Ideal Specimen Configuration for Total Hemispherical
Emittance Measurements

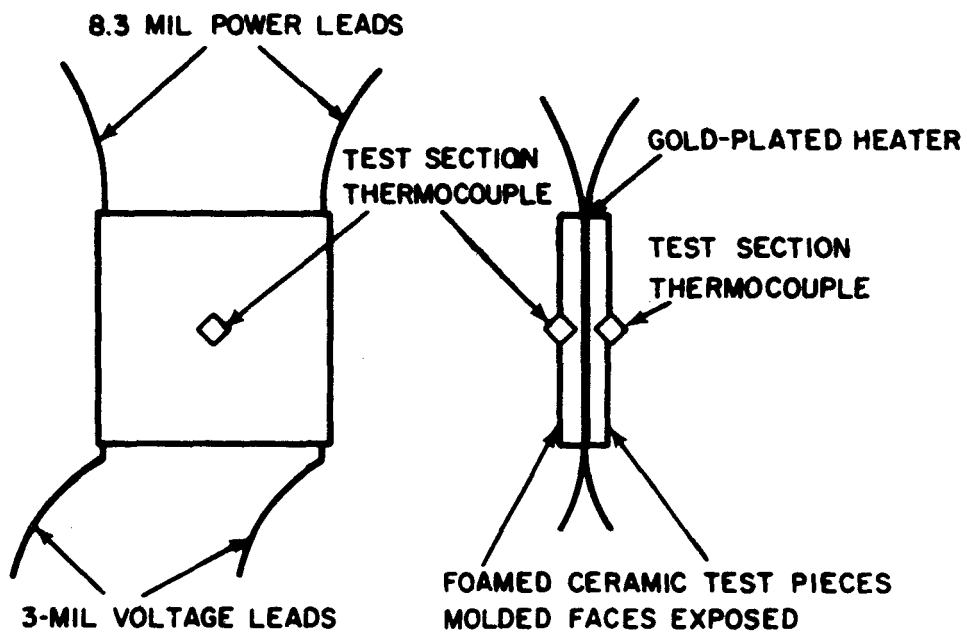


Figure 3. Configuration of First Total Hemispherical Emittance Specimen

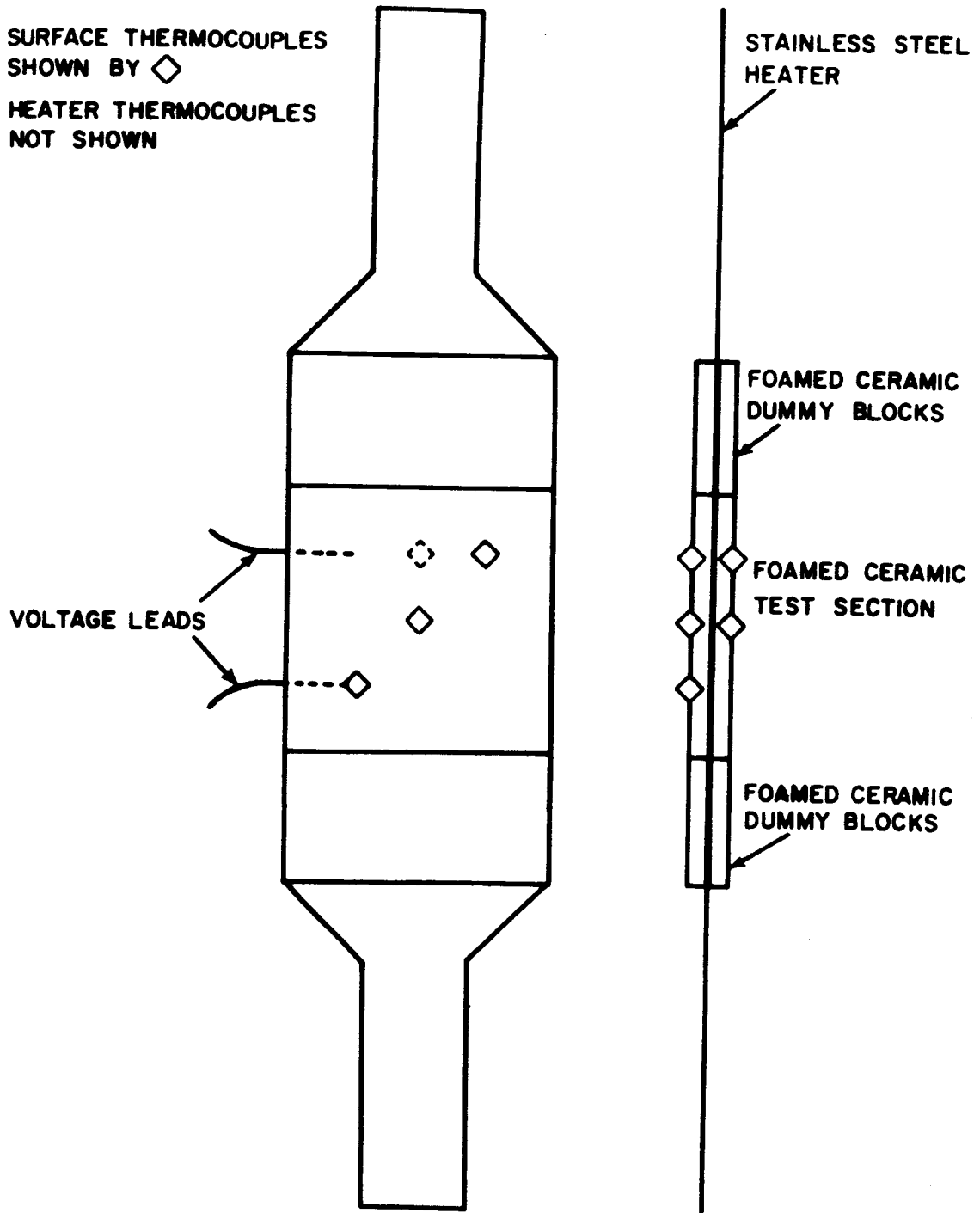


Figure 4. Configuration of Second Total Hemispherical Emittance Specimen